JACS
JOURNAL OF THE AMERICAN CHEMICAL SOCIETY

Article

pubs.acs.org/JACS

Metal Migration Processes in Homo- and Heterobimetallic Bismuth(III)−Lead(II) Porphyrin Complexes: Emergence of Allosteric Newton's Cradle-like Devices

Btissam Najjari, Stéphane Le Gac,* Thierry Roisnel, Vincent Dorcet, and Bernard Boitrel*

Université de Rennes 1, Institut des Sciences Chimiques de Rennes, UMR CNRS 6226, 263 avenue du Général Leclerc, CS 74205, 35042 Rennes Cedex, France

Supporting Information

ABSTRACT: Metal ion migration in a bis-strapped porphyrin ligand with overhanging carboxylate groups has been investigated in solution. Two types of homobimetallic complexes are generated with Pb(II) and Bi(III) cations, which stand on both sides of the macrocycle: (i) a dissymmetric complex with one cation bound to the porphyrin N core and the other cation hung over the N core through bonding with a carboxylate of a strap; (ii) a C_2-symmetric complex with both cations coordinated to the N core and to the carboxylate groups of the straps. Variable-temperature NMR studies and 2D rotational Overhauser effect spectroscopy NMR experiments have shown that in the former dissymmetric complexes, the two cations undergo a coupled intramolecular migration resulting in exchange of their coordination modes. Such complexes constitute active states of *Newton's cradle-like devices* (NCDs), with the ion migration rate depending on the lability of the metal−ligand interactions [Pb(II) faster than Bi(III) NCDs]. On the other hand, the C_2-symmetric complexes constitute either an inactive state [with Pb(II)] or a resting state [with Bi(III)] of an NCD, since they correspond respectively to a precursor or an intermediate in the motion of the cations. The NCDs are under both allosteric and acid−base control: (i) with Pb(II), the addition of an allosteric effector such as an acetate anion to the medium allows the conversion of the symmetric form to the dissymmetric one, thus triggering the Newton's cradle-like motion of the cations; (ii) with Bi(III), a lifted state was converted to a resting one by the addition of protons and then restored by the addition of a base. As an extension to nondegenerate systems, a heterobimetallic Bi(III)−Pb(II) complex was selectively obtained, and it constitutes a frozen lifted state of a dissymmetric NCD. All of these homo- and hetero-NCDs could be successively formed by selective metal ion exchange. These unique findings open the way to novel tristable devices.

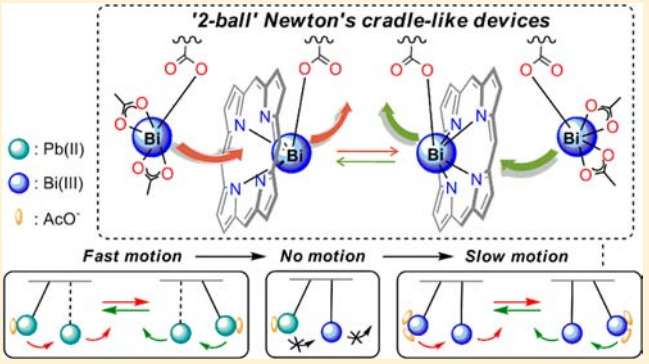

INTRODUCTION

Molecular switches based on transition-metal complexes have attracted considerable interest in the past decade, as they constitute promising prototypes of molecular devices and machines.[1,2] In such bistable systems, switching between two states can be achieved by a change in the coordination sphere of the metal ion triggered by an external stimulus (chemical, electrochemical, or photonic), thereby inducing a motion of some components of the system (shuttling, rotation, expansion, contraction, etc.) as found in rotaxane- and catenane-based devices. The two states of a bistable molecular switch can also arise from migration of a metal ion itself from one to another binding site of a ditopic ligand.[3] Early examples involved the redox-driven translocation of iron or copper centers in systems with hard and soft compartments.[3b,4] Protonation/deprotonation of a binding site is also a general way to induce migration of a metal center.[5] A higher degree of sophistication is represented by systems based on double translocation of metal ions, which are much less common. Fabbrizzi et al.[6] have produced a pH-dependent double translocation of two Cu(II) cations within a macrocyclic polydentate ligand, this process being a key feature for a receptor with adaptable behavior. With a ditopic calix[6]arene receptor, a redox-driven double translocation of two different metal ions (Cu and Zn) was recently reported by Reinaud and co-workers.[7] The further elaboration of devices based on bimetallic systems exhibiting switchable migration processes will require a thorough understanding of the metal motions and, for that, innovative ligands are desired.

Porphyrins and related macrocycles are likely to be one of the most versatile ligands in (bio)chemistry, with widespread utilization in the construction of functional supramolecular assemblies with applications in host−guest recognition and catalysis and for the elaboration of new materials and devices.[8] Most of these supramolecular systems are based on metalated macrocycles, and among the various strategies encountered in the supramolecular chemistry of metalloporphyrins, axial

Received: July 26, 2012
Published: September 4, 2012

   dx.doi.org/10.1021/ja307349d | J. Am. Chem. Soc. 2012, 134, 16017−16032

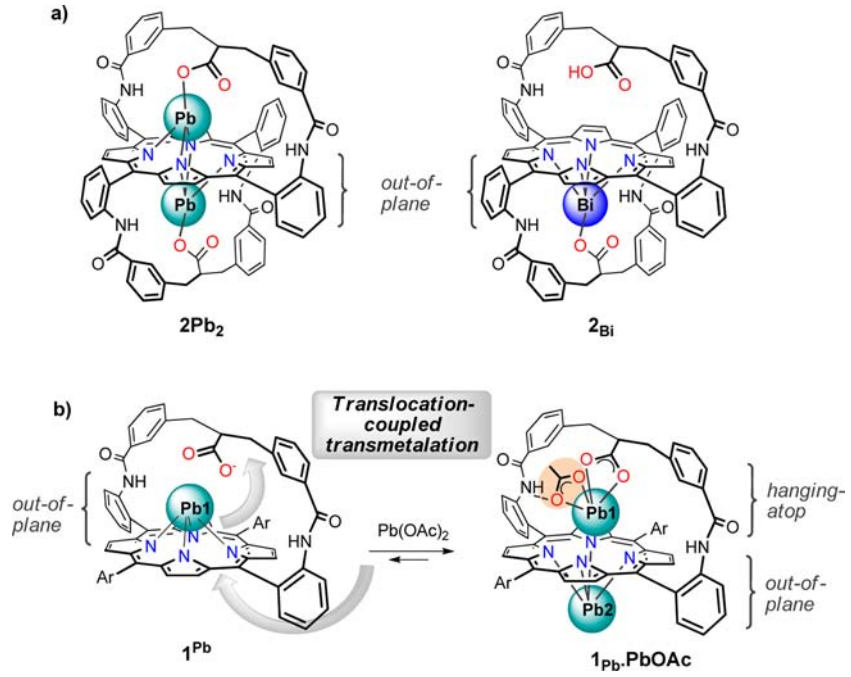

Figure 1. (a) Chemical structures of the homodinuclear lead(II) complex $\mathbf{2Pb_2}$ and the mononuclear bismuth(III) complex $\mathbf{2_{Bi}}$.[17] (b) Translocation-coupled transmetalation process leading to the homodinuclear lead(II) complex $\mathbf{1_{Pb}}$**·PbOAc** (Ar = 3,5-dimethoxyphenyl).[20]

ligation of an exogenous ligand to the metal cation bound in the porphyrin N core is the most popular. It is worth noting that very little attention, if any, has been paid to the dynamic binding of metal cations to the N core with the aim of engineering innovative molecular switches or devices integrating, for instance, transmetalation or translocation processes in their functioning. Transmetalation processes with porphyrins have been studied with the aim of increasing the rate of insertion of a metal ion.[9] A general mechanism involves the distortion of the porphyrin macrocycle induced by a large metal ion as a means to lower the activation free energy for the insertion of a smaller cation. The release of the first large metal ion, to the best of our knowledge, has not been exploited to date.

The various coordination types generated by the interaction of porphyrins with cations have long been known and classified for almost four decades.[10] With a regular porphyrin macrocycle, most of the metal complexes incorporate a single cation bound into the N core, with coordination spheres depending on the size of the cation and its interaction with additional ligands. Complexes with higher nuclearity (i.e., multimetallic species for which at least two metal ions interact with the N core) are much less common. These have been encountered in multiple-decker lanthanide complexes,[11] and a few examples involve a single porphyrin macrocycle. These are restricted to alkali-metal complexes derived from anionic transition-metal porphyrins[12] and to Re(I)/Tc(I)[13] and Tl(I)/Tl(I)[14] bimetallic complexes. This reluctance of the "naked" porphyrin to act as a bridging ligand is due to the restricted size and conformational mobility of the macrocycle and contrasts with the propensity of expanded or core-modified porphyrinoids to yield multimetal complexes.[15] In all of the above-mentioned examples, however, there was no specific design of the macrocycle, resulting in a lack of versatility. Conversely, appending a binding motif such as a carboxylic acid in the vicinity of the primary coordination site has proved to be a versatile strategy for the formation of bimetallic species with the period 6 main-group and late transition metals.[16] Such an environment allows the stabilization of unique homodinuclear complexes with Pb(II) (e.g., $\mathbf{2Pb_2}$ in Figure 1a)[17] and Hg(II) cations,[18] in which each metal ion is bound to both the N core and a hanging carboxylate group. High complexation rates under mild conditions, possibly with tunable cooperativity of the metal ion insertion process, are attractive features in further extending the frontiers of porphyrin supramolecular coordination chemistry.[19]

We recently described the use of this approach to form the homodinuclear lead porphyrin complex $\mathbf{1_{Pb}}$**·PbOAc** (Figure 1b), in which one of the lead cations (Pb1) is hung over the porphyrin core and "accommodated" in the dome-shaped porphyrin.[20,21] This *hanging-atop* (HAT) coordination mode requires (i) an acetate counteranion that is favorably oriented for a crucial H-bonding interaction with an amide group of the strap and (ii) a second metal ion (Pb2) coordinated to the N core of the macrocycle in an *out-of-plane* (OOP) fashion on the *opposite side* of the macrocycle relative to the intramolecular hanging carboxylate group. The latter condition is not easy to achieve, since it requires the stereoselective binding of a large cation to the porphyrin, a domain of research still unexplored. In $\mathbf{1_{Pb}}$**·PbOAc**, it was achieved by means of a translocation-coupled transmetalation mechanism, with an apparent *inside/outside* switching process of the N-core-bound Pb(II) cation when comparing the mono- and bimetallic complexes (Pb1 vs Pb2, respectively, in Figure 1b). Indeed, Pb2 approaches from the side opposite to Pb1, the latter being picked back up in a HAT coordination mode by the hanging COO^- under the specific condition of an exogenous AcO^- being present in the medium. Thus, although the HAT Pb(II) is not directly bound to the N core, its binding to the strap has a deep influence on the coordination of the other Pb(II) cation bound to the N core. Upon further exploration of this HAT coordination mode with other systems, it occurred to us that some related dynamic processes might take place with the C_2-symmetric complex

dx.doi.org/10.1021/ja307349d | J. Am. Chem. Soc. 2012, 134, 16017−16032

Scheme 1. Complexation Behavior of Ditopic Ligand 2 toward Pb(II) Cation[a]

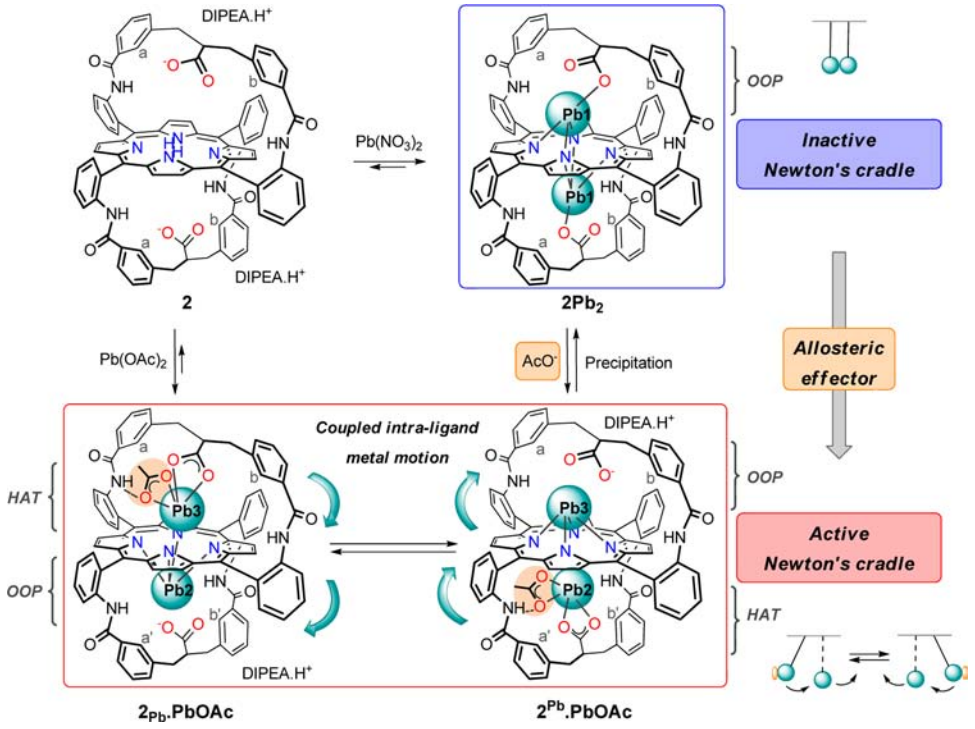

[a](top) In the absence of acetate anions, the C_2-symmetric dinuclear complex **2Pb$_2$** is readily formed and behaves as an inactive Newton's cradle-like device (NCD). (bottom) The binding of an acetate anion to one of the Pb ions modifies the coordination spheres of both metal centers, leading to a dissymmetric dinuclear complex that displays a Newton's cradle-like motion of the metal ions (bottom). HAT and OOP stand for hanging-atop and out-of-plane, respectively.

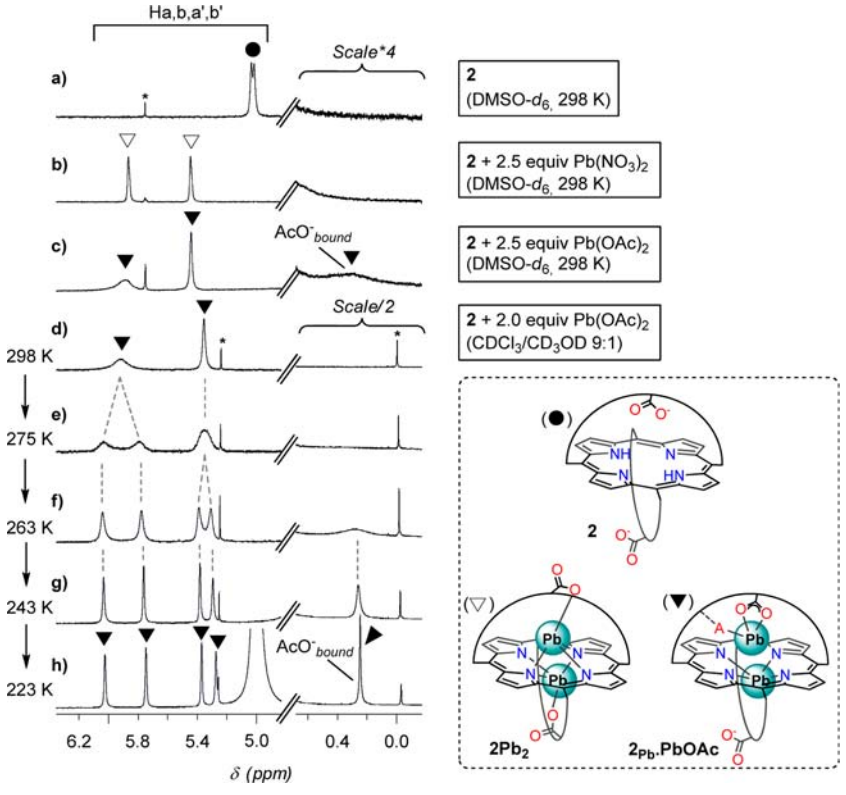

Figure 2. Partial ^{1}H NMR spectra (500 MHz) related to the study of Pb(II) complexation by ligand **2** in the presence of 15 equiv of DIPEA: (a–c) spectra of **2** recorded in DMSO-d_6 solution at 298 K (a) before and (b, c) after addition of 2.5 equiv of either (b) $Pb(NO_3)_2$ or (c) $Pb(OAc)_2$; (e–h) spectra of **2** in a 9:1 $CDCl_3/CD_3OD$ solution upon addition of 2 equiv of $Pb(OAc)_2$ at (d) 298, (e) 275, (f) 263, (g) 243, and (h) 223 K. * labels denote peaks due to solvent or grease. Inset: structures of the ligand **2** and the complexes **2Pb$_2$** and **2$_{Pb}$·PbOAc**. "A" stands for AcO^-.

dx.doi.org/10.1021/ja307349d | J. Am. Chem. Soc. 2012, 134, 16017–16032

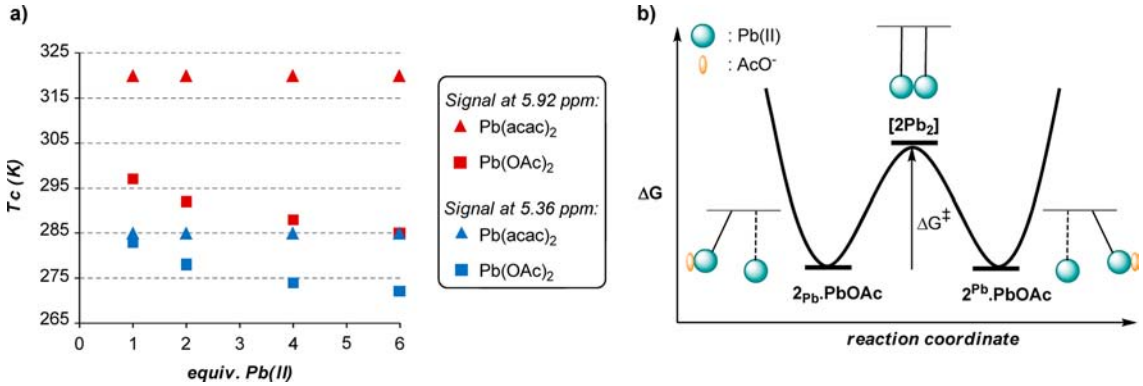

Figure 3. (a) Concentration dependence of the coalescence temperatures (T_c) for the signals $H_a \leftrightarrow H_{a'}$ and $H_b \leftrightarrow H_{b'}$ in complex $\mathbf{2_{Pb}}$**·PbOAc** ($[\mathbf{2}]_0 = 0.47 \times 10^{-3}$ mol L^{-1}, 9:1 $CDCl_3/CD_3OD$, 15 equiv of DIPEA) upon addition of $Pb(OAc)_2$ or $Pb(acac)_2$. In the case of $Pb(acac)_2$, 4 equiv of tetrabutylammonium acetate were previously added, so only the concentration of Pb(II) cation was varied. (b) Idealized free energy profile for the Newton's cradle-like motion of the Pb(II) cations in the bimetallic complex $\mathbf{2_{Pb}}$**·PbOAc**.

$2Pb_2$ (Figure 1a), which bears the same straps. We also turned our attention to the previously described mononuclear bismuth(III) complex $\mathbf{2_{Bi}}$ (Figure 1a).[17,22] In this complex, the trivalent cation is OOP-bound to the porphyrin N core with one of the hanging carboxylate groups as an intramolecular counteranion. Therefore, the Bi atom sits on the *opposite side* of the macrocycle relative to the remaining free carboxylic acid, and this situation is precisely one of the requirements for the binding of a HAT Pb(II) cation. Herein we describe the formation and dynamic behavior of Pb(II) and Bi(III) homo- and heterobimetallic complexes derived from the bis-overhanging carboxylate ligand **2** that exhibit a unique intramolecular coupled migration process of interest for the construction of innovative molecular switches.[23]

RESULTS AND DISCUSSION

Dynamic Features of Pb(II) Homodinuclear Complexes. The complexation behavior of ligand **2** toward Pb(II) cation was investigated by ^{1}H NMR spectroscopy in perdeuterated dimethyl sulfoxide (DMSO-d_6) solution in the presence of diisopropylethylamine (DIPEA, 15 equiv). Ligand **2** was first titrated with a solution of $Pb(NO_3)_2$ [see the Supporting Information (SI)]. Equilibria were reached instantaneously at 298 K, and the solution turned deep green right after the addition of Pb(II). The titration evidenced a highly cooperative process for lead insertion into **2**, as the C_2-symmetric complex **$2Pb_2$** was the only observable species quantitatively formed upon addition of 2 equiv of $Pb(NO_3)_2$ (Scheme 1 top). No trace of a possible mononuclear complex was detected, as a 1:1 ratio of **2** and **$2Pb_2$** was observed after the addition of 1 equiv of the metal salt.[24] This drastically differs from the complexation behavior of ligand **1**, for which mono- and dinuclear species are successively formed. The ^{1}H NMR spectrum of **$2Pb_2$** formed under those conditions is well-defined at 298 K (Figure 2b) and very similar to that of the isolated complex.[17] The titration was repeated under the same experimental conditions with a solution of $Pb(OAc)_2$ (see the SI), which led to the same behavior but with a significantly broadened ^{1}H NMR pattern of the dinuclear species with a notable new signal at ca. 0.30 ppm (Figure 2, panel c vs b). This chemical shift matches that of the bound acetate of $\mathbf{1_{Pb}}$**·PbOAc**.[20] The signal of the free acetate anions at 1.78 ppm was also large, indicating their implication in an exchange process. Hence, the dinuclear species displays some fluxionality in the presence of acetate anions. A variable-temperature NMR study in a 9:1 $CDCl_3/CD_3OD$ solution revealed a similar broadening of the ^{1}H NMR pattern of the dinuclear species at 298 K (Figure 2d). Low-temperature measurements (Figure 2e–h) evidenced a single species with a dissymmetric pattern, with four singlets for protons H_a, H_b, $H_{a'}$, and $H_{b'}$ in the 5–6 ppm region instead of two singlets as for **2** or **$2Pb_2$** formed with $Pb(NO_3)_2$ (the proton labeling is shown in Scheme 1). Also, a sharp singlet accounting for three protons appeared at 0.24 ppm with decreasing temperature (Figure 2f–h) and was attributed to a bound acetate counteranion on the basis of 2D heteronuclear multiple-quantum coherence (HMQC), heteronuclear multiple-bond correlation (HMBC), and rotational Overhauser effect spectroscopy (ROESY) NMR experiments (δ_{CH_3} = 23.8 ppm and δ_{CO} = 176.1 ppm; see the SI). These data indicate that the two sides of the porphyrin bind Pb(II) cations in different coordination modes. The upfield shift of 1.60 ppm for the CH_3 protons of the bound acetate is similar to that observed in the case of the related dinuclear species $\mathbf{1_{Pb}}$**·PbOAc** with a HAT Pb(II) cation (1.60 ppm in DMSO-d_6 at 298 K) and is due to the location of this counteranion above the porphyrin plane. Therefore, the dinuclear species formed upon addition of lead acetate to **2** likely corresponds to complex $\mathbf{2_{Pb}}$**·PbOAc** (Scheme 1 bottom), in which one Pb(II) cation is bound to the N core of the macrocycle in an OOP geometry while the other is hung above the porphyrin plane in the HAT coordination mode. High-resolution mass spectrometry (HRMS) analysis gave further evidence for the formation of this complex,[25] which is actually the two-strap analogue of $\mathbf{1_{Pb}}$**·PbOAc**.

The coalescence of the signals, leading to a broad C_2-symmetric NMR signature at 298 K, indicates an exchange of the coordination modes of the Pb(II) cations between the OOP and HAT coordination geometries. In other words, an equilibrium between $\mathbf{2_{Pb}}$**·PbOAc** and $\mathbf{2^{Pb}}$**·PbOAc** (Scheme 1 bottom) does exist and is fast on the NMR time scale at room temperature.[26] Formally, these findings could be explained in one of two ways: (i) through an intermolecular pathway that would require the successive decomplexation and recomplexation of *both* metal ions (i.e., formal exchange of Pb2 and Pb3) or (ii) through an intramolecular pathway via coupled migration of the metal ions with exchange of the acetate counteranion, in which Pb2 and Pb3 remain on their respective sides of the porphyrin. The first explanation is very unlikely. In

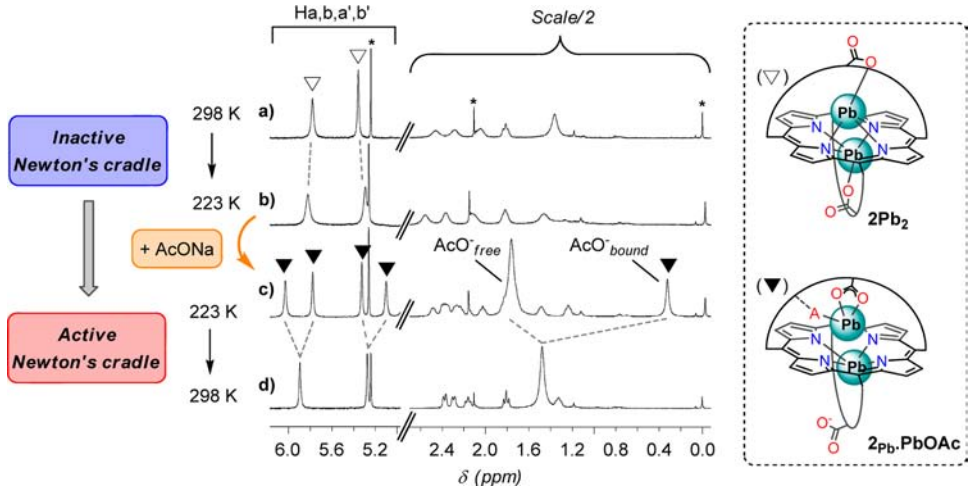

Figure 4. NMR study evidencing an allosteric Newton's cradle-like device: ^{1}H NMR spectra (9:1 $CDCl_3/CD_3OD$, 500 MHz) of (a, b) the isolated complex **2Pb$_2$** at (a) 298 and (b) 223 K and (c, d) after addition of 4 equiv of AcONa at (c) 223 and (d) 298 K. For proton labeling, see Scheme 1. * indicates solvent or grease peaks. In the inset showing the structures, "A" stands for AcO^-.

the case of exchange of the Pb(II) cations according to an intermolecular pathway that is fast on the NMR time scale, one would expect an average spectrum of **2** and **2$_{Pb}$·PbOAc** at 298 K, which is not the case [see the titration experiment with $Pb(OAc)_2$ in the SI; the coalescence temperature for the equilibrium between these two species is higher than 373 K in DMSO-d_6]. In addition, **2$_{Pb}$·PbOAc** is quantitatively formed upon the addition of 2 equiv of $Pb(OAc)_2$, which indicates high binding strength. Decomplexation of both Pb(II) cations would be energetically costly and therefore not favored at all. Conversely, an intramolecular translocation-coupled transmetalation process involving the Pb(II) cations (Scheme 1, green arrows) that is similar to the intermolecular process observed for the formation of the related dinuclear complex **1$_{Pb}$·PbOAc** (Figure 1b) would have a lower energetic cost. Such a process can be described formally as follows (Scheme 1 bottom, from left to right): translocation of the OOP Pb2 cation from the N core to the strap, with concomitant binding of an acetate counteranion, is coupled to the reverse process for the HAT Pb3 cation, namely, translocation from the strap to the N core, with concomitant release of the bound Pb3 acetate counteranion.

To obtain further insights into this mechanism, we examined the effect of the metal salt concentration on the coalescence temperature (T_c). First, T_c values were measured upon addition of increasing amounts of $Pb(OAc)_2$ to a solution of **2** (Figure 3a, squares). A significant decrease of 10−15 K was observed upon addition of 1−6 equiv of the metal salt. This concentration dependence of T_c reflects an intermolecular event. Second, T_c values were measured at a fixed concentration of acetate anions. For that, 4 equiv of tetrabutylammonium acetate was added to **2**, followed by increasing amounts of $Pb(acac)_2$.[27] Under those conditions, the T_c values were not affected by the changes in the concentration of Pb(II) cations (Figure 3a, triangles). These data are in full agreement with intramolecular coupled migration of the Pb(II) cations in going from **2$_{Pb}$·PbOAc** to **2^{Pb}·PbOAc**, this process being associated with an intermolecular pathway for exchange of the bound acetate. Consequently, the results also strongly suggest that the C_2-symmetric complex **2Pb$_2$** formed as a stable species in the absence of acetate takes part in this exchange process as a transition state intermediate (Figure 3b). From the X-ray structures of **2Pb$_2$**[17] and **1$_{Pb}$·PbOAc**,[20] the distances of a Pb atom to the 24-atom mean plane (24MP) of the porphyrin are 1.795, 2.323, and 1.383 Å in **2Pb$_2$** and for the HAT and OOP Pb atoms in **1$_{Pb}$·PbOAc**, respectively. Thus, the positions of the Pb atoms in **2Pb$_2$** are midway between those expected in **2$_{Pb}$·PbOAc**. Therefore, both the enthalpy and entropy of activation are expected to be low (see below).

The inherent, coupled intraligand motion of the Pb(II) cations in **2$_{Pb}$·PbOAc** is reminiscent of the motion of spheres in the well-known Newton's cradle device.[28] The process of translocation from HAT to OOP coordination resembles the motion of a sphere released from a lifted position. Similarly, the coupled process of going from OOP to HAT coordination resembles that of a sphere pushed up into the symmetrically opposite lifted position. Therefore, the bimetallic complex **2$_{Pb}$·PbOAc** can be viewed as the first example of a "two-ball" *Newton's cradle-like device* (NCD). This complex can be described as an active state of an NCD, and conversely, the C_2-symmetric complex **2Pb$_2$** would be an inactive or sleeping state of an NCD (no HAT coordination, no lifted sphere) (Scheme 1). On the basis of the above-mentioned Pb−24MP distances, a magnitude of ca. 1 Å would be expected for the intraligand motion of a Pb(II) cation.

A parallel can be drawn with the inherent dynamics of degenerate [2]rotaxanes (systems possessing two identical stations that allow a shuttling motion of a macrocycle)[29] or, for example, with the tunneling motion of a Ag(I) cation in a ditopic 1,3-alternate calix[4]arene,[30] as the potential energy surface is symmetric (ΔG = 0, so the two states of such molecular shuttles/switches are equally populated). However, in the present NCD system, the switching process is not purely intramolecular, as the exchange of an acetate counteranion from one to the other metal ion proceeds through an intermolecular pathway. Figure 3b shows an idealized free energy profile of the Newton's cradle-like motion, for which the rate of metal ion motion is determined by the free energy of activation ($\Delta G^{\ddagger}$). The activation parameters were assessed from the T_c values for four different ^{1}H NMR signals using the Eyring equation and found to be $\Delta H^{\ddagger}$ = 12.3 kcal mol^{-1}, $\Delta S^{\ddagger}$ = −4.9 cal mol^{-1} K^{-1}, and $\Delta G^{\ddagger}_{298K}$ = 13.7 kcal mol^{-1} (see the SI). The latter value corresponds to a rate of 534 s^{-1} and thus to a frequency of ca. 500 swings of the cradle per second at room temperature. The

dx.doi.org/10.1021/ja307349d | J. Am. Chem. Soc. 2012, 134, 16017−16032

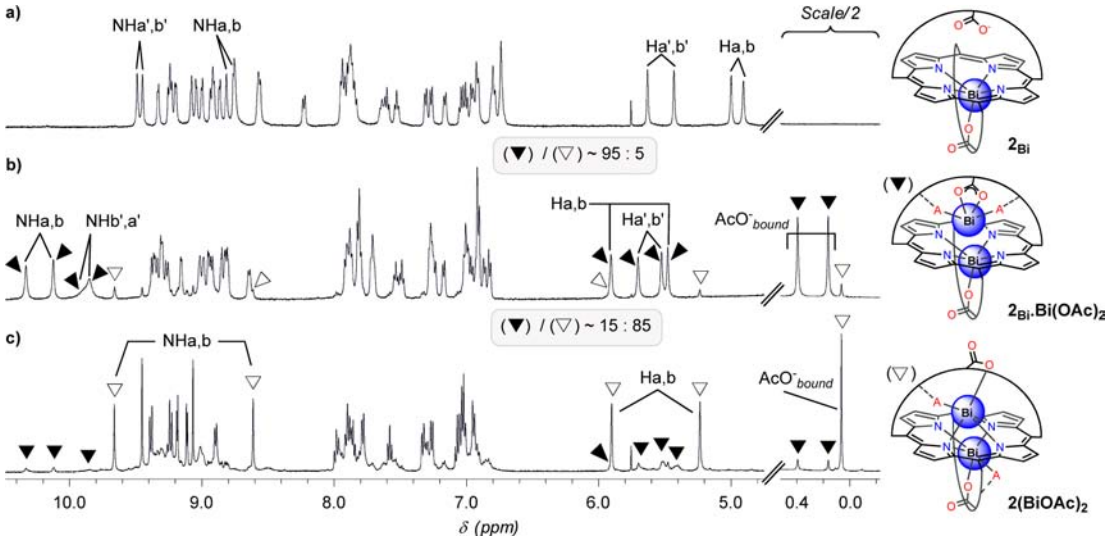

Figure 5. ^{1}H NMR spectra (500 MHz, 298 K) of the complexes (b) $\mathbf{2_{Bi}{\cdot}Bi(OAc)_2}$ and (c) $\mathbf{2(BiOAc)_2}$ formed as the major species by the addition of excess of $Bi(OAc)_3$ to (a) $\mathbf{2_{Bi}}$ in DMSO-d_6 solution in the presence (15 equiv) and absence of DIPEA, respectively. Equilibria were reached instantaneously at 298 K. For proton labeling, see Scheme 2. In the inset, "A" stands for AcO^-.

Scheme 2. Formation of Coordination Isomers $\mathbf{2_{Bi}{\cdot}Bi(OAc)_2}$ and $\mathbf{2(BiOAc)_2}$ upon Addition of Bismuth(III) Acetate to the Bismuth Complex $\mathbf{2_{Bi}}$ in DMSO-d_6 Solution[a]

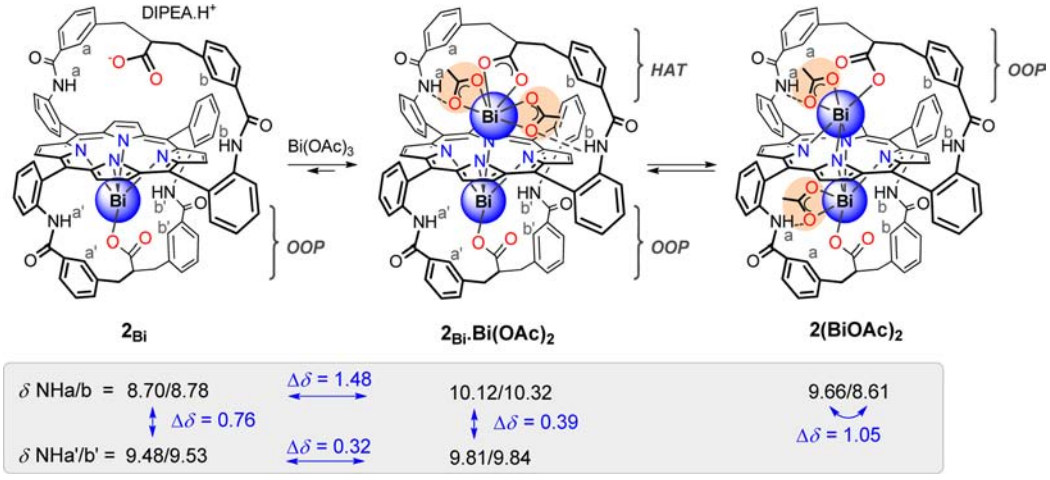

[a]The ratio of these two homobimetallic complexes depends on the presence of a base (DIPEA; see the text and Figure 5). Inset: chemical shifts (in ppm) of the NHCO protons in the mono- and bimetallic complexes; δ_{NH} are given in presence of excess of DIPEA (15 equiv); $\Delta\delta$ (absolute values) are average values for protons NH_a/NH_b (and $NH_{a'}/NH_{b'}$).

enthalpy of activation is on the order of the energy needed to break 2−3 H-bonds, which argues well for $\mathbf{2Pb_2}$ as the transition state in the Newton's cradle-like motion. In addition to the breaking of H-bonds, the activation enthalpy probably also reflects the inversion of the distorted (mainly dome-shaped) porphyrin ring.

All attempts to isolate complex $\mathbf{2_{Pb}{\cdot}PbOAc}$ remained unsuccessful. Rather surprisingly, precipitation of this complex in a methanol/water mixture led to the release of the acetate counteranion and formation of $\mathbf{2Pb_2}$ (Scheme 1 right). Indeed, the isolated complex displayed a C_2-symmetric NMR signature at both 298 and 223 K (Figure 4a,b), with no signal of acetate anions observed. Interestingly, the addition of few equivalents of AcO^- in the NMR tube solution led to a dissymmetric NMR pattern at 223 K (Figure 4c), with two new signals corresponding to free and bound acetates (1.76 and 0.32 ppm, respectively; assigned through 2D HMBC and HMQC experiments). This spectrum corresponds to the formation of complex $\mathbf{2_{Pb}{\cdot}PbOAc}$, which, as expected, displays a C_2-symmetric NMR signature at room temperature (average spectrum; Figure 4d). These NMR data evidence an allosteric process. Upon addition of AcO^- to the inactive NCD $\mathbf{2Pb_2}$, the coordination spheres of both Pb(II) cations are affected even though AcO^- binds to only one of the metal centers. This leads to an active state of the NCD, complex $\mathbf{2_{Pb}{\cdot}PbOAc}$, in which coupled intraligand motion of the Pb(II) cations occurs. Hence, AcO^- behaves as an allosteric effector that "lifts up" a sphere (i.e., induces the HAT coordination mode) and activates the device (Scheme 1 right). To the best of our knowledge, such an allosteric NCD is unique.

The inherent dynamics of such a homodinuclear complex is a general feature of degenerate systems with two identical states. To explore further the NCD mechanism as a new entry in the field of molecular switches, we were interested in breaking the

dx.doi.org/10.1021/ja307349d | J. Am. Chem. Soc. 2012, 134, 16017−16032

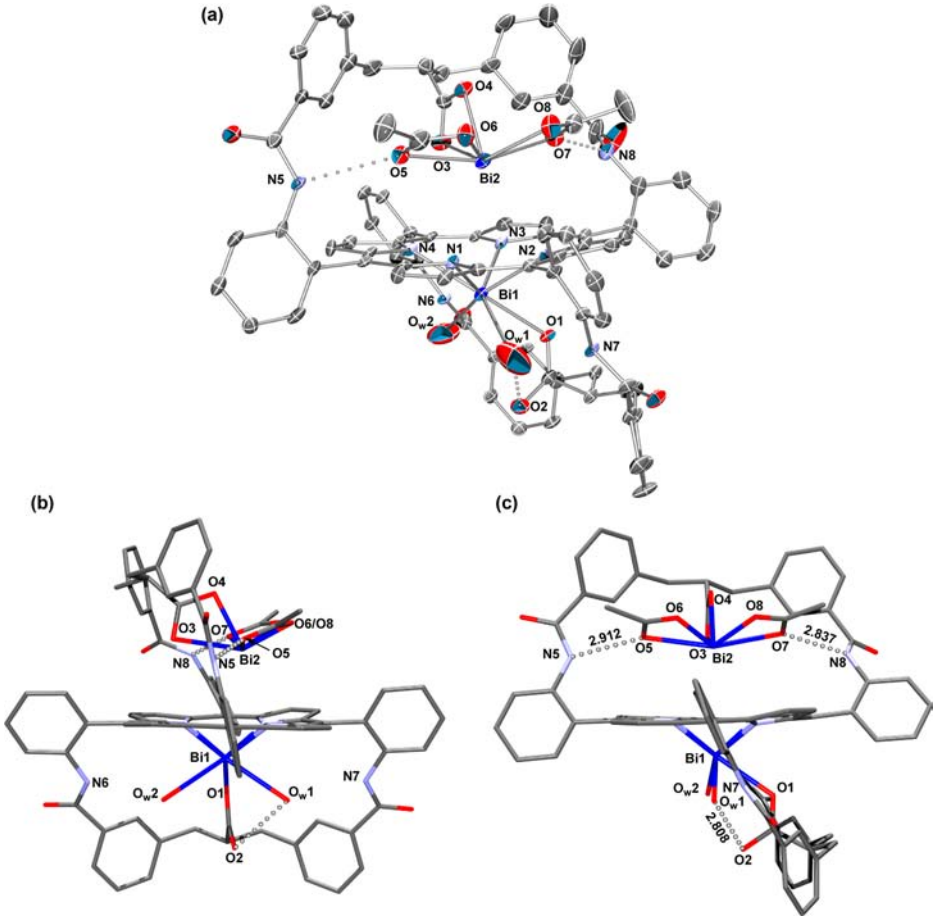

Figure 6. X-ray structure of $\mathbf{2_{Bi}}\cdot\mathbf{Bi(OAc)_2}$ (H atoms removed for clarity). (a) ORTEP perspective view (30% probability level). (b) Rod side view orthogonal to the strap coordinating Bi2. (c) Rod side view orthogonal to the strap coordinating Bi1. Selected distances (Å): Bi1−24MP, 1.310; Bi2−24MP, 2.576; Bi1−Bi2, 3.932; N1−Bi1, 2.429; N2−Bi1, 2.306; N3−Bi1, 2.331; N4−Bi1, 2.442; O1−Bi1, 2.491; O3−Bi2, 2.493; O4−Bi2, 2.212; O5−Bi2, 2.487; O6−Bi2, 2.292; O7−Bi2, 2.551; O8−Bi2, 2.260.

symmetry of the bimetallic system and therefore, we designed an NCD with two different metal ions. In a next step, the complexation behavior of ligand **2** toward a trivalent metal ion was examined.

Dynamic Features of Bi(III) Homodinuclear Complexes. Complex $\mathbf{2_{Bi}}$ (Figure 1a) was prepared as described previously,[17] and its binding properties toward Bi(III) cations were investigated by ^{1}H NMR spectroscopy in DMSO-d_6 solution. In contrast to the C_2-symmetric NMR pattern of the free base, that of $\mathbf{2_{Bi}}$ is dissymmetric and displays four singlets in the 5−6 ppm region for the H_a, H_b, $H_{a'}$, and $H_{b'}$ protons (Figure 5a; see Scheme 2 for labeling). We observed that the ^{1}H NMR pattern of $\mathbf{2_{Bi}}$ was slightly affected by the addition of excess of $Bi(NO_3)_3$, suggesting some weak interactions. Further addition of NaOAc to that mixture led to a broadened NMR pattern distinct from that of $\mathbf{2_{Bi}}$. We anticipated that a second bismuth cation might also interact in a HAT fashion, this process being driven by the acetate counteranions in a manner similar to what was observed with Pb(II). Well-resolved ^{1}H NMR spectra were obtained using $Bi(OAc)_3$ instead of $Bi(NO_3)_3$ (Figure 5). Two sets of signals corresponding to the formation of two species were observed, and the ratio of these species was strongly dependent on the presence of a base. In the presence of DIPEA (15 equiv), the addition of excess of $Bi(OAc)_3$ to $\mathbf{2_{Bi}}$ followed by sonication led to a ca. 95:5 ratio of these new complexes (Figure 5b, solid and open triangles). The major species displays a dissymmetric NMR pattern, with upfield-shifted singlets at 0.39 and 0.16 ppm accounting for three protons each. They were attributed to two acetate anions on the basis of ROESY and HMQC 2D NMR experiments (see the SI). The upfield shifts of 1.41 and 1.64 ppm for these CH_3 protons relative to those of the free acetates are close to the shifts observed for a HAT PbOAc moiety (ca. 1.60 ppm for $\mathbf{1_{Pb}}\cdot\mathbf{PbOAc}$ and $\mathbf{2_{Pb}}\cdot\mathbf{PbOAc}$) and thus indicate similar positioning of these counteranions above the porphyrin plane. In addition, nuclear Overhauser effect (NOE) cross-peaks were observed between these CH_3 signals at 0.39 and 0.16 ppm and the β-pyrrolic protons at 8.95 and 9.02 ppm, respectively (see the SI). These data are in agreement with the binding of a HAT Bi(III) cation to $\mathbf{2_{Bi}}$ and the formation of the bimetallic complex $\mathbf{2_{Bi}}\cdot\mathbf{Bi(OAc)_2}$ (Scheme 2). Elemental analysis of an analytical sample provided further evidence for the bimetallic nature of this complex.[25] It is noteworthy that two of the four NHCO protons appear as sharp singlets (δ_{NH} = 10.32 and 10.12 ppm) and are downfield-shifted by ca. 1.48 ppm upon complexation of the HAT Bi(III) cation (Scheme 2).[31] They are also downfield-shifted by ca. 0.39 ppm relative to the two other NHCO signals in the bimetallic complex (broad singlets at δ_{NH} = 9.84 and 9.81 ppm) (Scheme 2). This indicates that both acetate counteranions of the HAT Bi(III) are H-bonded to the amide groups of the strap.

dx.doi.org/10.1021/ja307349d | J. Am. Chem. Soc. 2012, 134, 16017−16032

We were able to grow crystals of $\mathbf{2_{Bi}{\cdot}Bi(OAc)_2}$ from a chloroform/cyclohexane mixture. The complex crystallized in the triclinic space group $P\bar{1}$, and the structure confirmed the homodinuclear nature of this species, in which two bismuth atoms coexist but only one of them (Bi1) is directly bound to the N core of the porphyrin (Figure 6).[32] This bismuth cation is related to its counterpart observed in $\mathbf{2_{Bi}}$. Bi1 is seven-coordinate and 1.310 Å out of the 24MP, with an average N−Bi1 bond length of 2.375 Å. It is also bound to a hanging carboxylate group of the strap in a monohapto fashion (O1−Bi1 = 2.494 Å) and to two water molecules (O_w1 and O_w2), one of which (O_w1) is stabilized by H-bonding with the O2 atom of the hung carboxylate group (O_w1−O2 = 2.839 Å). It is worth noting that the locations of the OOP Bi(III) cations in $\mathbf{2_{Bi}}$ and $\mathbf{2_{Bi}{\cdot}Bi(OAc)_2}$ are the same (1.309 Å and 1.310 Å, respectively) and that almost no difference in the dome-shaped conformation of the macrocycle could be detected (see the SI). The second bismuth cation (Bi2) is coordinated on the opposite side of the porphyrin but without any direct interaction with the N core (Bi2−24MP = 2.576 Å; average N−Bi2 distance = 3.409 Å). Indeed, it is bound in a bishapto mode to the overhanging carboxylate group (O3/O4) and to two acetate counteranions (O5/O6 and O7/O8). These latter are maintained by H-bonds with the amide groups of the strap (N5−O5 = 2.843 Å and N8−O7 = 2.911 Å). The plane of each acetate group is almost perpendicular to that of the intramolecular carboxylate group, thereby defining a strongly hemidirected coordination sphere of Bi2 with an *inward* orientation. Whether this unusual geometry for a six-coordinate Bi(III) cation originates from possible activity of the $6s^2$ lone pair of bismuth[33] or arises from a strong chelate effect of the strapped ligand, or both, is under investigation. These data, together with the previously reported structure of the dinuclear Pb(II) complex $\mathbf{1_{Pb}{\cdot}PbOAc}$,[20] evidence a versatile coordination site made of a carboxylate group hung over the concave face a dome-shaped metalloporphyrin; this site can accommodate either a HAT PbOAc or a HAT $Bi(OAc)_2$ moiety, with the second coordination sphere playing a crucial role.

As mentioned above, a minor species was detected together with $\mathbf{2_{Bi}{\cdot}Bi(OAc)_2}$ in the presence of a base, but its low proportion hampered attribution of its NMR pattern. Interestingly, when $Bi(OAc)_3$ was added to a DMSO-d_6 solution of $\mathbf{2_{Bi}}$ in the absence of DIPEA, this minor species became the major one and $\mathbf{2_{Bi}{\cdot}Bi(OAc)_2}$ the minor one, in an observed ratio of ca. 85:15 (Figure 5c). In contrast to $\mathbf{2_{Bi}}$ and $\mathbf{2_{Bi}{\cdot}Bi(OAc)_2}$, this species displayed a C_2-symmetric NMR pattern, as evidenced by, for example, two singlets at 5.90 and 5.23 ppm attributed to the H_a and H_b protons. The fact that both sides of the porphyrin are identical indicates the binding of a second bismuth cation, with both cations adopting the same coordination mode. In addition, an upfield-shifted singlet at 0.06 ppm accounting for six protons was attributed to acetate anions on the basis of a ROESY 2D NMR experiment. Again, the upfield shift of 1.81 ppm for the acetate protons relative to the free ones indicates a position above the macrocycle. These data strongly suggest the binding of a BiOAc moiety on both sides of the porphyrin, affording the C_2-symmetric complex $\mathbf{2(BiOAc)_2}$ (Scheme 2). The downfield shift of 1.05 ppm for protons NH_a versus NH_b also indicates H-bonding interactions of the acetate counteranions with one of the amide groups of the strap.

The homobimetallic complexes $\mathbf{2_{Bi}{\cdot}Bi(OAc)_2}$ and $\mathbf{2(BiOAc)_2}$ are coordination isomers and the trivalent analogues of complexes $\mathbf{2_{Pb}{\cdot}PbOAc}$ and $\mathbf{2Pb_2}$, respectively. The ROESY spectrum of the mixture of these bismuth complexes displayed exchange correlations between these two species, and it was therefore intriguing to study the dynamics of this system. Variable-temperature NMR studies were undertaken with complex $\mathbf{2_{Bi}{\cdot}Bi(OAc)_2}$ as the major species (up to 408 K in DMSO-d_6). Ill defined spectra were obtained with no clear coalescence, indicating that a dissociative mechanism might operate at high temperature. More interesting data came from the ROESY spectrum of a 95:5 mixture of $\mathbf{2_{Bi}{\cdot}Bi(OAc)_2}$ and $\mathbf{2(BiOAc)_2}$ (see the SI). Similarly to Pb(II), we found that the same Bi(III) cation in the complex $\mathbf{2_{Bi}{\cdot}Bi(OAc)_2}$ adopts alternatively the HAT and OOP coordination modes. Indeed, exchange correlations were observed between the signals of the "C_2-symmetry-related" protons of the two straps (Figure 7).

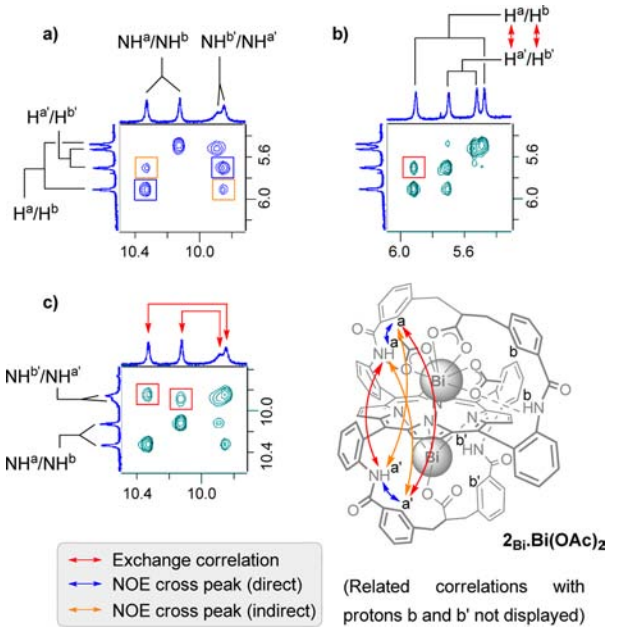

Figure 7. Selected correlations observed in the 2D ROESY spectrum (δ in ppm) of a 95:5 mixture of $\mathbf{2_{Bi}{\cdot}Bi(OAc)_2}$ and $\mathbf{2(BiOAc)_2}$ (DMSO-d_6 solution, 15 equiv of DIPEA): (a) NOE cross-peaks; (b, c) exchange correlations.

For instance, exchange correlations occurred exclusively between protons H_a (H_b) and $H_{a'}$ ($H_{b'}$) and also between protons NH_a (NH_b) and $NH_{a'}$ ($NH_{b'}$) (red arrows in Figure 7b,c, respectively). As a result, in addition to the expected NOE cross-peak between, for example, protons NH_a and H_a (Figure 7, blue arrows), an indirect NOE cross-peak was observed between NH_a and $H_{a'}$ (Figure 7, orange arrows).[34] Similarly, an indirect NOE cross-peak occurred between protons $NH_{a'}$ and H_a (Figure 7, orange arrows). These data evidence an exchange of the two metal binding sites (i.e., an interconversion of the HAT and OOP coordination modes) that, for the following reasons, must arise from an intramolecular mechanism involving an equilibrium with $\mathbf{2(BiOAc)_2}$:

(i) Exchange of the OOP and HAT Bi(III) cations through intermolecular processes (i.e., through equilibria with the monometallic complex $\mathbf{2_{Bi}}$ and the free base **2**) would require decomplexation of both cations with a high energetic cost; this is unlikely to occur since $\mathbf{2_{Bi}{\cdot}Bi(OAc)_2}$ is formed starting from the isolated complex $\mathbf{2_{Bi}}$.

dx.doi.org/10.1021/ja307349d | J. Am. Chem. Soc. 2012, 134, 16017−16032

(ii) The ROESY spectrum of the mononuclear complex $\mathbf{2_{Bi}}$ formed in situ by addition of 1 equiv of $Bi(OAc)_3$ to **2** (DMSO-d_6, 15 equiv of DIPEA) did not show any exchange correlation between the protons of the two straps (see the SI). Also, in the case of a ~ 2:1 mixture of $\mathbf{2_{Bi}}$ and **2**, no exchange correlation between the signals of these two species was observed. This indicates a high residence time of the Bi(III) cation in $\mathbf{2_{Bi}}$, in line with the strong stability of the complex[17,23] with no exchange of the metal center between the two sides of the ligand.

Therefore, following the example of $\mathbf{2_{Pb}}$**·PbOAc**, a Newton's cradle-like intramolecular motion for the apparent exchange of the two Bi(III) cations in $\mathbf{2_{Bi}}$**·Bi(OAc)$_2$** is proposed (Figure 8a). Formally, translocation of one Bi(III) cation from the strap

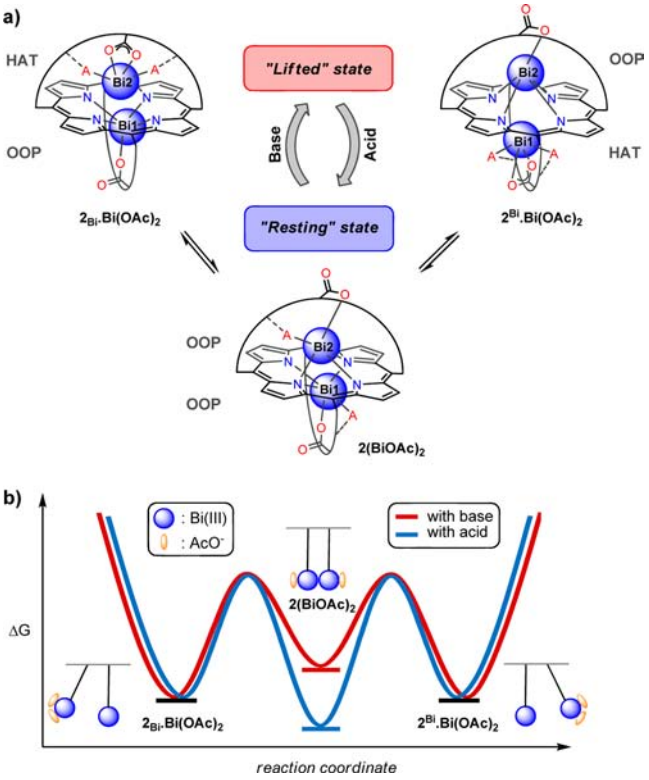

Figure 8. (a) Acid–base-controlled, bistable NCD formed by homobimetallic Bi(III) complexes derived from **2** ("A" stands for AcO^-). (b) Idealized free energy profile for the coupled migration of the Bi(III) cations.

to the N core (i.e., from HAT to OOP coordination) is coupled to the reverse process for the other Bi(III) cation, namely, translocation from the N core to the other strap (i.e., from OOP to HAT coordination). During this process, an apparent switch of the OOP N-core-bound Bi(III) cation from one to the other side of the macrocycle occurs (i.e., $\mathbf{2_{Bi}} \leftrightarrow \mathbf{2^{Bi}}$). From a mechanistic point of view, this intramolecular exchange (from left to right in Figure 8a) requires the binding of an acetate anion to Bi1 and the removal of one from Bi2, thus leading to **2(BiOAc)$_2$**. The further binding of an acetate anion to Bi1 and the departure of the bound acetate on Bi2 generates the complex $\mathbf{2^{Bi}}$**·Bi(OAc)$_2$**, which is formally identical to $\mathbf{2_{Bi}}$**·Bi(OAc)$_2$** but has the two Bi(III) cations in opposite coordination modes. In contrast to the parent Pb(II) NCD, for which the C_2-symmetric complex $\mathbf{2Pb_2}$ is likely a transition state (Figure 3b), the C_2-symmetric complex **2(BiOAc)$_2$** is an intermediate species observed in solution. In other words, the coupled migration of the Bi(III) cations occurs through a two-step process, for which an idealized free energy profile is displayed Figure 8b. Hence, the lifted and resting states coexist in solution. It is noteworthy that the slower metal motion displayed by this Bi(III) NCD in comparison with its Pb(II) analogue is in line with the stronger stability of bismuth versus lead complexes. For instance, $\mathbf{2Pb_2}$ and $\mathbf{2_{Pb}}$**·PbOAc** are rapidly demetalated on silica gel, whereas $\mathbf{2_{Bi}}$ tolerates a large excess of trifluoroacetic acid (TFA). Hence, the more labile complex swings faster.

DIPEA deeply influences the selective formation of one of the coordination isomers $\mathbf{2_{Bi}}$**·Bi(OAc)$_2$** and **2(BiOAc)$_2$** over the other, although its exact role is still poorly understood. Interestingly, we further observed that these complexes are fully interconvertible in solution, as shown by the following results summarized in Figure 9. First, the bimetallic complex **2(BiOAc)$_2$** was formed as the major species by addition of $Bi(OAc)_3$ to a DMSO-d_6 solution of $\mathbf{2_{Bi}}$ in the absence of a base (Figure 9a,b). Second, addition of DIPEA afforded the coordination isomer $\mathbf{2_{Bi}}$**·Bi(OAc)$_2$**, and subsequent addition of TFA restored the complex **2(BiOAc)$_2$** (Figure 9c,d). With a larger excess of TFA, selective demetalation of one bismuth cation occurred, giving the monometallic complex $\mathbf{2_{Bi}}$ (Figure 9e). Finally, addition of excess DIPEA led to the successive formation of **2(BiOAc)$_2$** and $\mathbf{2_{Bi}}$**·Bi(OAc)$_2$** (Figure 9f,g). These data nicely evidence a unique coordination behavior: (i) a Bi(III) cation can adopt three different coordination modes, tuned by the presence of a base, when taking part in homobimetallic porphyrin complexes; (ii) the same Bi(III) cation can switch between two different coordination modes in the same complex. In this set of experiments, a full cycle between three different states (off, resting, and lifted; Figure 9) was achieved through acid–base amplification of one or the other coordination isomer (Figure 8a). The major difference with the parent Pb(II) NCD, which is present in either an inactive state ($\mathbf{2Pb_2}$, no acetate) or an active state ($\mathbf{2_{Pb}}$**·PbOAc**, triggered by acetate), is that the populations of the resting and lifted states [**2(BiOAc)$_2$** and $\mathbf{2_{Bi}}$**·Bi(OAc)$_2$**, both part of an active NCD] in the case of Bi(III) can be tuned (Figure 8b). This gives an additional possibility in the design of NCD-based switches.

Breaking the Symmetry: Selective Formation of a Bi(III)–Pb(II) Heterodinuclear Complex. The next degree of sophistication involved the design of a dissymmetric NCD as an extension to nondegenerate systems. For that, we investigated the complexation behavior of **2** toward a mixture of Pb(II) and Bi(III) cations. In the case of a heteroselective process (i.e., the selective formation of a heterodinuclear Bi–Pb complex), three possibilities can be envisioned according to the above studies, corresponding to three different states of a dissymmetric NCD (Scheme 3): a "bismuth lifted state" with HAT coordination of Bi(III) and OOP coordination of Pb(II), a "resting state" with OOP coordination of both both Bi(III) and Pb(II), and a "lead lifted state" with OOP coordination of Bi(III) and HAT coordination of Pb(II).

The binding properties of complex $\mathbf{2_{Bi}}$ toward Pb(II) were investigated by ^{1}H NMR spectroscopy in DMSO-d_6 solution without DIPEA. Whereas addition of excess of $Pb(NO_3)_2$ or $PbCl_2$ led only to minor effects on the NMR spectrum of $\mathbf{2_{Bi}}$, this complex was fully consumed upon addition of 1 equiv of $Pb(OAc)_2$ (Figure 10a–c). The corresponding NMR spectrum is characterized by four broad singlets for the H_a, H_b, $H_{a'}$, and

dx.doi.org/10.1021/ja307349d | J. Am. Chem. Soc. 2012, 134, 16017–16032

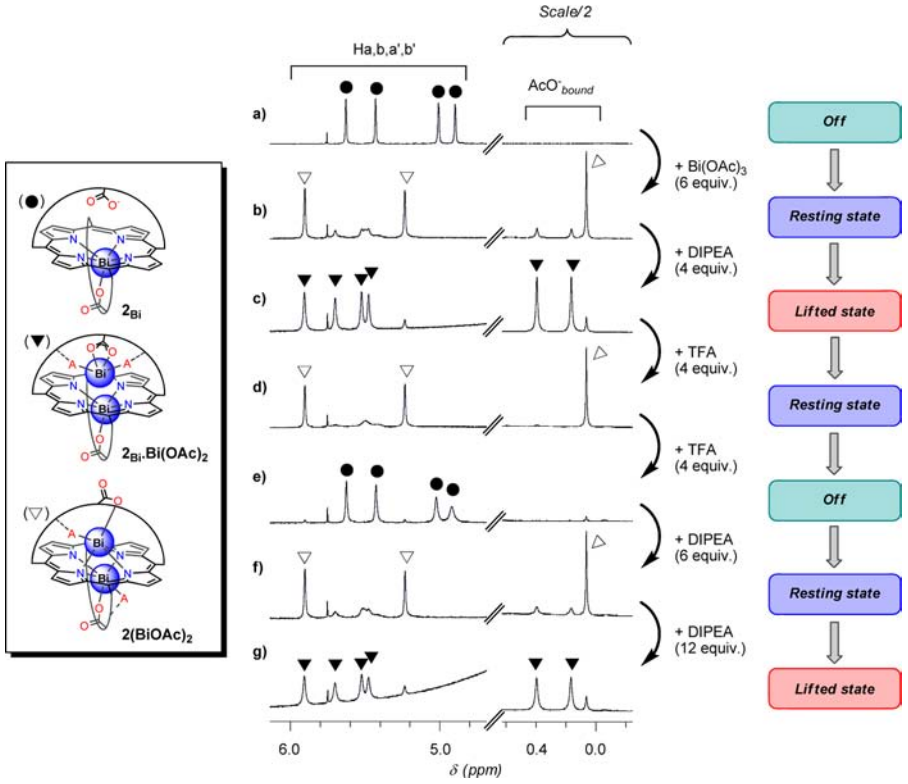

Figure 9. ^{1}H NMR study (500 MHz, DMSO-d_6, 298 K) of the acid–base-controlled interconversion of mono- and bimetallic Bi(III) complexes derived from **2**: (a) $\mathbf{2}_{Bi}$; (b) upon addition of excess of $Bi(OAc)_3$ and sonication; (c) upon addition of DIPEA; (d, e) upon addition of TFA; (f, g) upon further addition of DIPEA. In the inset, "A" stands for AcO^-. Equilibria were reached instantaneously.

Scheme 3. Schematic Representation of Three Possible Heterodinuclear Bi(III)–Pb(II) Complexes Derived from Ligand 2

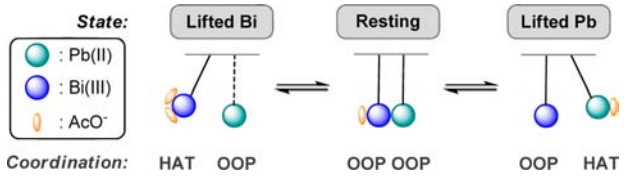

$H_{b'}$ protons (for labeling, see Scheme 4), in agreement with the formation of a dissymmetric species. No traces of the Pb(II) and Bi(III) homobimetallic species derived from **2** were observed (see the reference spectra in Figure 10d,e), indicating a highly selective process to form a heterobimetallic complex. A broad signal of three protons was also observed at 0.36 ppm, consistent with a single acetate bound to this species (assigned on the basis of a ROESY 2D NMR experiment; see the SI). From these NMR data, the formation of the Bi–Pb heterobimetallic complex with the Bi(III) cation in the HAT coordination mode ("Lifted Bi" in Scheme 3) is excluded. The coordination isomers called "Resting" and "Lifted Pb" in Scheme 3 both incorporate a single acetate counteranion and thus cannot be easily distinguished. However, the chemical shift of 0.36 ppm for the bound acetate (Figure 10c) is much closer to that of a PbOAc moiety (ca. 0.30 ppm for $\mathbf{2}_{Pb}$**·PbOAc**) than that of a BiOAc moiety [0.06 ppm for $\mathbf{2(BiOAc)_2}$]. Thus, the spectrum of Figure 10c is expected to correspond to the heterobimetallic complex $\mathbf{2}_{Bi}$**·PbOAc** (Scheme 4), with OOP and HAT coordination of Bi(III) and Pb(II), respectively ("Lifted Pb" in Scheme 3). This hypothesis was supported by

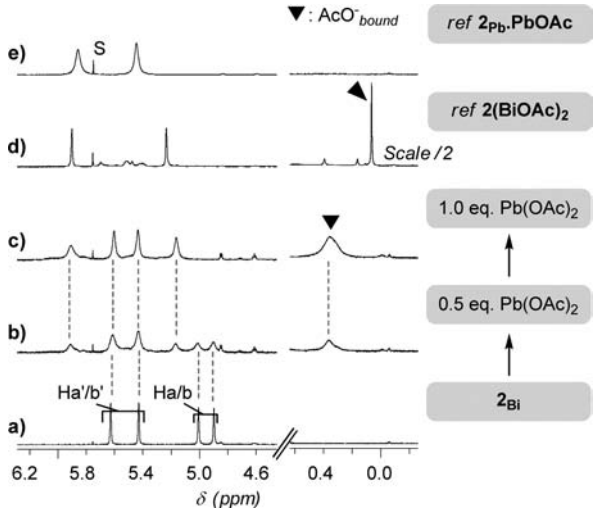

Figure 10. (a–c) Partial ^{1}H NMR spectra for the addition of $Pb(OAc)_2$ to $\mathbf{2}_{Bi}$ (DMSO-d_6, 298 K) and (d, e) reference ^{1}H NMR spectra of the homodinuclear complexes $\mathbf{2(BiOAc)_2}$ and $\mathbf{2}_{Pb}$**·PbOAc**. Equilibria were reached instantaneously; for proton labeling, see Scheme 4. The label "S" indicates a solvent peak.

an X-ray structure obtained from single crystals grown upon slow evaporation of the NMR tube (Figure 11).

The complex crystallized as dark-green crystals in the monoclinic space group *C*2/*c*. The structure confirmed the heterodinuclear Bi(III)–Pb(II) complex $\mathbf{2}_{Bi}$**·PbOAc**, with the bismuth and lead cations located on opposite sides of the porphyrin (Bi–Pb = 3.802 Å) and only the bismuth cation bound to the porphyrin N core (Figure 11a). The coordination

dx.doi.org/10.1021/ja307349d | J. Am. Chem. Soc. 2012, 134, 16017–16032

Scheme 4. Complexation Behavior of Complex 2_{Bi} toward Pb(II) in DMSO-d_6, Leading to the Heterodinuclear Complex 2_{Bi}·PbOAc

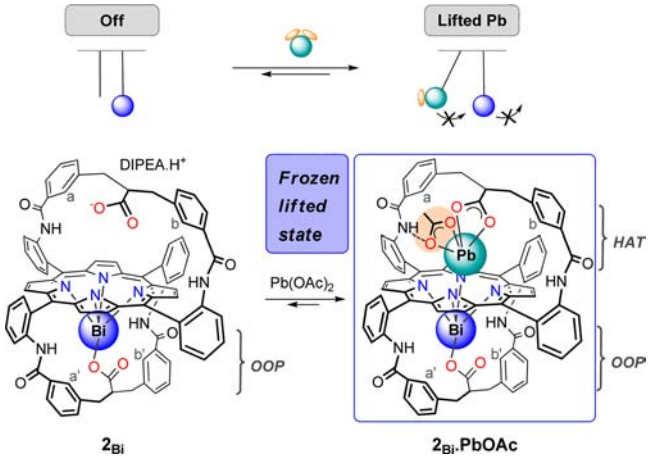

modes of bismuth and lead acetate are very similar to those encountered in $\mathbf{2_{Bi}}$, $\mathbf{2_{Bi}}$·$\mathbf{Bi(OAc)_2}$, and $\mathbf{1_{Pb}}$·**PbOAc** and coexist in the same ligand with a remarkable degree of complementarity. On one side, the bismuth cation is seven-coordinate, 1.559 Å out of the 24MP in an antiprismatic polyhedron. It is bound to the four nitrogen atoms of the macrocycle and to the hanging carboxylate group of the strap in a monohapto fashion. The coordination sphere is completed with two molecules of DMSO maintained by H-bonds with the amide groups of the straps (dashed lines in Figure 11b). On the other side, the lead cation adopts an *inward* orientation, with a strongly hemidirected coordination sphere due to the stereochemically active Pb lone pair, as in $\mathbf{1_{Pb}}$·**PbOAc**. The Pb(II) ion is at the apex of a distorted pyramid composed of an intramolecular carboxylate counterion from the strap, an exogenous acetate counteranion (both bound in a bishapto fashion), and a DMSO ligand. The acetate and DMSO are perpendicular to the intramolecular carboxylate and are stabilized by H-bonds with the amide groups of the strap (dashed lines in Figure 11c). Lead is hung over the 24MP at a height of 2.231 Å and does not interact with the N core (average N−Pb = 3.115 Å). On the basis of our previous study,[20] the Pb lone pair is assumed to point toward the N core of the macrocycle.

Direct comparison of the HAT Pb(II) geometries in $\mathbf{2_{Bi}}$·**PbOAc** and the related complex $\mathbf{1_{Pb}}$·**PbOAc** was done by superimposition of their X-ray structures (see the SI). This operation evidenced strong similarities in both the position and coordination sphere of the hung PbOAc moiety and in the conformation of the strap binding Pb(II). In other words, the HAT Pb(II) is almost insensitive to the nature of the second metal ion bound to the N core on the opposite side [i.e., four-coordinate Pb(II) vs seven-coordinate Bi(III) with an intramolecular counteranion]. The distortion of the porphyrin induced by these two large cations is indeed roughly the same.

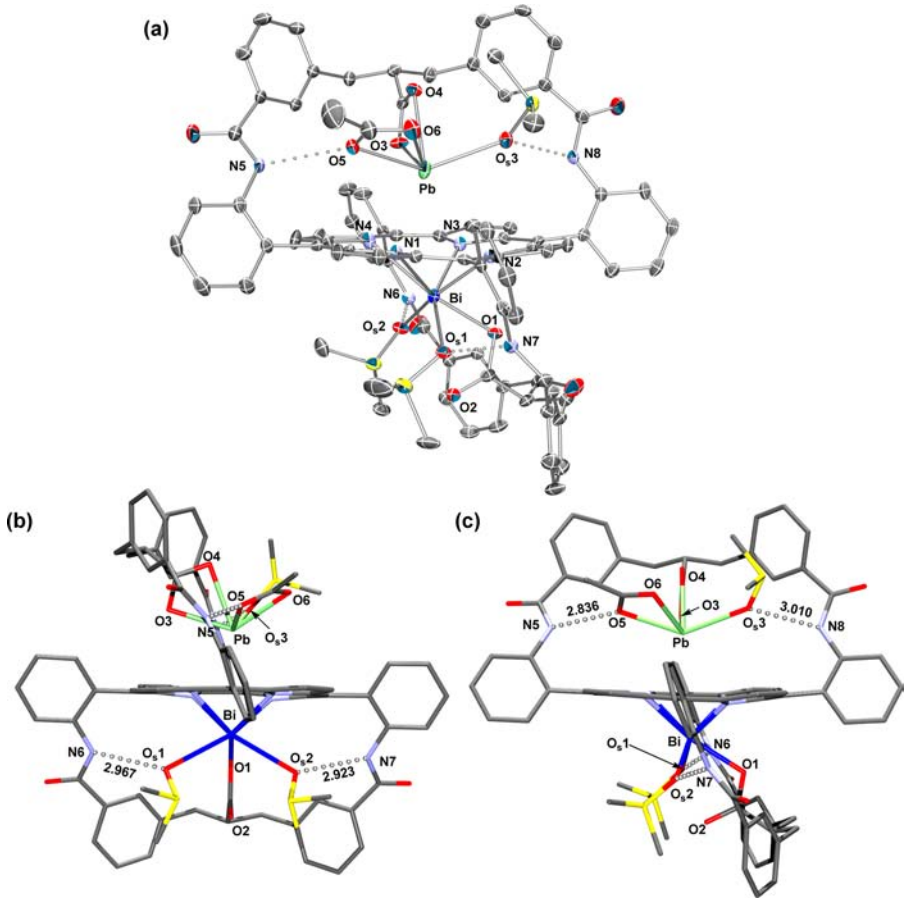

Figure 11. X-ray structure of $\mathbf{2_{Bi}}$·**PbOAc** (H atoms removed for clarity). (a) ORTEP perspective view (30% probability level). (b) Rod side view orthogonal to the strap coordinating Pb(II). (c) Rod side view orthogonal to the strap coordinating Bi(III). Selected distances (Å): Bi−24MP, 1.559; Pb−24MP, 2.231; Bi−Pb, 3.802; N1−Bi, 2.638; N2−Bi, 2.342; N3−Bi, 2.393; N4−Bi, 2.678; O1−Bi, 2.294.

dx.doi.org/10.1021/ja307349d | J. Am. Chem. Soc. 2012, 134, 16017−16032

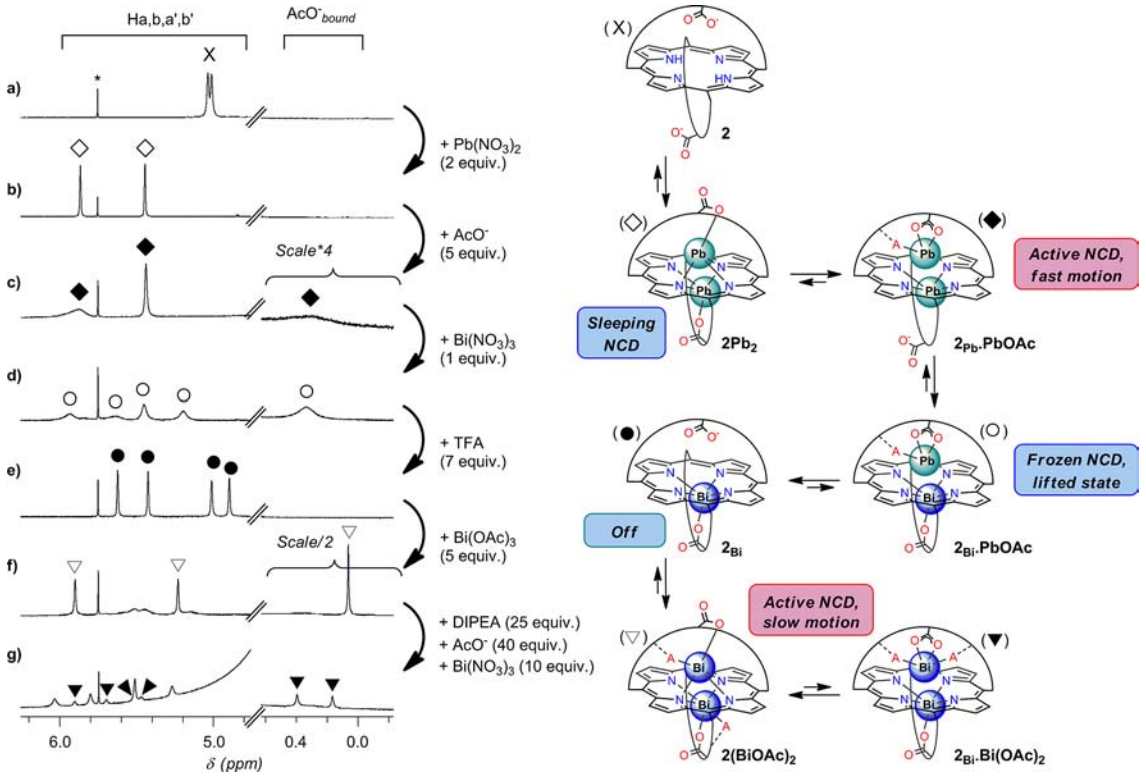

Figure 12. ^{1}H NMR spectra (500 MHz, DMSO-d_6, 298 K) corresponding to the successive formation of six different metal complexes derived from (a) **2**: (b) $\mathbf{2Pb_2}$, (c) $\mathbf{2_{Pb}{\cdot}PbOAc}$, (d) $\mathbf{2_{Bi}{\cdot}PbOAc}$, (e) $\mathbf{2_{Bi}}$, (f) $\mathbf{2(BiOAc)_2}$, and (g) $\mathbf{2_{Bi}{\cdot}Bi(OAc)_2}$.

The second coordination sphere, and notably the key H-bond between the acetate counteranion and the NHCO group of the strap, are almost identical ($d_{O-N} \approx 2.9$ Å in both cases). Similarly, the coordination spheres of the N-core-bound Bi atoms in $\mathbf{2_{Bi}{\cdot}PbOAc}$ and the parent complexes $\mathbf{2_{Bi}}$ and $\mathbf{2_{Bi}{\cdot}Bi(OAc)_2}$ were also compared (see the SI). A significant difference in the OOP position was observed, as Bi is located 1.559 Å from the 24MP in $\mathbf{2_{Bi}{\cdot}PbOAc}$ versus 1.309 Å in $\mathbf{2_{Bi}}$ and 1.310 Å in $\mathbf{2_{Bi}{\cdot}Bi(OAc)_2}$. The distortion of the porphyrin appears to be similar in these three complexes, but the average N−Bi distance is slightly longer in $\mathbf{2_{Bi}{\cdot}PbOAc}$ [2.513 vs 2.388 Å in $\mathbf{2_{Bi}}$ and 2.375 Å in $\mathbf{2_{Bi}{\cdot}Bi(OAc)_2}$]. These data reflect some repulsive electrostatic interaction between the two metal cations [HAT Pb(II) and OOP Bi(III)] in a more constrained environment, the HAT Pb atom being closer to the 24MP in $\mathbf{2_{Bi}{\cdot}PbOAc}$ than the HAT Bi atom in $\mathbf{2_{Bi}{\cdot}Bi(OAc)_2}$ (2.231 vs 2.575 Å, respectively).

These structural data indicate that the two coordination modes of both bismuth and lead nicely fit together into the same ligand with remarkable complementarity. The "recoil" of the OOP Bi in the heterobimetallic complex evidences communication between the two binding sites of the ditopic ligand (N core and strap). Again, the binding of the HAT Pb(II) is possible because of the OOP binding of Bi(III) on the opposite side, which distorts the porphyrin, and the presence of an acetate counteranion favorably oriented for H-bonding with the strap.

Various experimental conditions for the binding of Pb(II) to $\mathbf{2_{Bi}}$ were explored, and we did not find any evidence for an equilibrium with other possible heterobimetallic complexes such as those drawn in Scheme 3.[35] It therefore seems that $\mathbf{2_{Bi}{\cdot}PbOAc}$ constitutes a frozen lifted state of a dissymmetric NCD or, said differently, an inactive NCD with a lifted sphere (Scheme 4). This behavior constitutes a major difference between the heterobimetallic system and the parent Pb(II) and Bi(III) homobimetallic NCDs (degenerate systems), which present an inherent coupled migration of the cations when one of them adopts the HAT coordination mode. From NMR studies under similar experimental conditions, complex $\mathbf{2_{Bi}{\cdot}PbOAc}$ was also formed upon addition of $Bi(OAc)_3$ and $Pb(OAc)_2$ to the free base **2** independent of the order of introduction of the metal ions, and therefore, the formation process is under thermodynamic control. The process leading to $\mathbf{2_{Bi}{\cdot}PbOAc}$ is highly selective, as no other species was observed with excess Bi(III) and Pb(II) cations (5 equiv each). The higher stability of the HAT Pb(II) cation versus Bi(III) is rather surprising, as both acetate anions in the case of Bi(III) are stabilized by H-bonds with the amide groups of the strap. This could be ascribed to better preorganization of the PbOAc moiety in comparison with $Bi(OAc)_2$ due to the more active $6s^2$ lone pair of Pb, resulting in a higher degree of complementarity with the binding site. More detailed investigations are obviously needed to substantiate this. Interestingly, the binding of HAT-coordinated Pb(II) was also found to be subject to acid−base control: addition of excess TFA to $\mathbf{2_{Bi}{\cdot}PbOAc}$ led to the selective decomplexation of the lead cation and formation of $\mathbf{2_{Bi}}$, while subsequent addition of excess DIPEA led to full recovery of $\mathbf{2_{Bi}{\cdot}PbOAc}$ (see the SI).

Selective Metal Ion Exchanges for the Successive Formation of Six Different Pb(II)/Bi(III) Metal Complexes. As a further example of the versatility of this system, we attempted to form successively in the same NMR tube all of the above-described complexes derived from **2** (Figure 12). Starting from a solution of **2** in DMSO-d_6 in the presence of 5 equiv of DIPEA, addition of lead(II) nitrate (2 equiv) and then tetrabutylammonium acetate (5 equiv) led successively to

the homodinuclear complexes **2Pb$_2$** and **2$_{Pb}$·PbOAc** (Figure 12a–c). Subsequent addition of 1 equiv of bismuth(III) nitrate led to the selective exchange of the OOP-coordinated Pb(II) cation to form the heterodinuclear complex **2$_{Bi}$·PbOAc** (Figure 12d). Further addition of TFA led to the selective decomplexation of the Pb(II) cation, giving **2$_{Bi}$** (Figure 12e). Upon addition of excess of bismuth(III) acetate, the C_2-symmetric complex **2(BiOAc)$_2$** was obtained quantitatively (Figure 12f). Finally, addition of excess DIPEA, tetrabutylammonium acetate, and bismuth(III) nitrate afforded **2$_{Bi}$·Bi(OAc)$_2$** as a minor species (Figure 12g, nonoptimized conditions). Hence, the equilibria among the mononuclear and homo- and heterodinuclear complexes can be easily shifted and proceed instantaneously at room temperature. This holds good promises if one wants to tune the rate of an NCD by selective metal ion exchange (Figure 12 right).

CONCLUSION

In summary, a unique intramolecular coupled migration process involving two metal cations has been evidenced in Pb(II) and Bi(III) homobimetallic complexes derived from a bis-strapped porphyrin ligand with an overhanging carboxylate group on each side of the N core. These complexes incorporate a metal cation on each side of the macrocycle, and an inherent coupled metal motion occurs under the conditions that one of the cations adopts the so-called *hanging-atop* (HAT) coordination mode. In this process, the two cations exchange their coordination modes: translocation of a HAT Pb(II) or Bi(III) cation from its binding strap to the N core is coupled to the reverse process for the other cation, a formal translocation from the N core to the other strap. An N-core-bound cation is thus artificially switched from one side to the other. The rate of the metals' motion depends on the involved metal center: the more labile metal ion exhibits faster motion (Pb > Bi). This particular process is reminiscent of the motion of spheres in the well-known Newton's cradle device, in which a sphere released from its lifted position induces an opposite motion of a symmetrically related sphere upon collision. In the present Newton's cradle-like devices, the coupled motion of the metal ions can be induced (allosteric control) or tuned (acid–base control):

- In the case of Pb(II), a C_2-symmetric homobimetallic complex is formed in the absence of acetate anions, and hence, no metal motion occurs. The binding of an acetate anion to one of the Pb(II) cations modifies the coordination spheres of both metal ions and generates an active NCD, as one of the Pb(II) displays a HAT coordination mode. Hence, acetate acts as an allosteric effector that "lifts up a sphere" and induces the inherent coupled motion of the cations.
- In the case of Bi(III), two coordination isomers coexist in solution and are part of a two-step NCD: a C_2-symmetric homobimetallic complex that constitutes a resting state [no HAT Bi(III) cation] and a dissymmetric homobimetallic complex with a HAT Bi(III) cation that constitutes a lifted state. The population of these two states is under acid–base control, and a full switching cycle involving three species (mono and bimetallic) was achieved.

In the case of the heterobimetallic Bi–Pb complex, in which Bi(III) and Pb(II) are bound to the N core and in HAT coordination mode, respectively, no intramolecular metal motion occurs. Thus, a dissymmetric NCD is selectively formed and appears as frozen in a "Pb lifted" state. Selective metal ion exchange in solution was also demonstrated, with up to six different complexes being successively formed. Thus, triggering the NCD (*inactive* → *fast motion*) and tuning the rate of swinging (*fast motion* → *frozen* → *slow motion*) can be easily done.

As revealed by the X-ray structures of the homobimetallic Bi(III) and heterobimetallic Bi(III)/Pb(II) complexes, the key points of these versatile NCDs are the following:

(i) OOP coordination of a large metal ion from the opposite side of an overhanging carboxylate, hence mimicking a stereoselective metalation. This results in a dome-shaped macrocycle that can "accommodate" a second cation in a HAT coordination mode.

(ii) A second sphere of coordination that involves H-bonding between the metal bound acetate(s) and the amide group(s) of the strap. This stabilizes the HAT coordination mode.

(iii) Several interdependent activation phenomena allowing dynamic processes. These include deconvolution of a metal salt by an overhanging carboxylate group, which allows fast metalation and translocation processes, and distortion of the macrocycle induced by OOP coordination of a large cation. The latter process is reminiscent of the distortion-induced metal insertion mechanism displayed by chelatases.[36].

Together, these results open new perspectives in supramolecular coordination chemistry with metalloporphyrins and related macrocycles, particularly in the field of molecular switches. On the basis of these findings, we are currently investigating various ligands and metal ions, trying to identify fully switchable tristable NCDs.

EXPERIMENTAL SECTION

General. All of the NMR experiments were conducted in 5 mm standard NMR tubes. ^{1}H NMR spectra were recorded at 500 MHz. Chemical shifts are expressed in parts per million, and traces of residual solvents were used as internal standards. All of the ^{1}H NMR signals were assigned using 2D NMR experiments (COSY, HMQC, ROESY). For ROESY experiments, different mixing times ranging from 75 to 750 ms were used. Compound **2** and complex **2$_{Bi}$** were prepared as previously described.[17] All of the chemicals were commercial products and used as received.

Procedures for the Formation of Complexes 2$_{Pb}$·PbOAc, 2$_{Bi}$·Bi(OAc)$_2$, 2(BiOAc)$_2$, and 2$_{Bi}$·PbOAc. The complex **2$_{Pb}$·PbOAc** was prepared by mixing 3.0 mg of **2** (2.38 μmol), 500 μL of 9:1 $CDCl_3/CD_3OD$, 6 μL of DIPEA (34.4 μmol, 15 equiv), and 80 μL (4.77 μmol, 2 equiv) of a stock solution of $Pb(OAc)_2{\cdot}3H_2O$ (11.3 mg in 500 μL of 9:1 $CDCl_3/CD_3OD$). The ^{1}H NMR spectrum recorded at 223 K showed the quantitative formation of **2$_{Pb}$·PbOAc**.

The complex **2$_{Bi}$·Bi(OAc)$_2$** was prepared from a solution of 3.5 mg of **2$_{Bi}$** (2.39 μmol) in 500 μL of DMSO-d_6 to which 6 μL of DIPEA (34.4 μmol, 15 equiv) and 4.6 mg of $Bi(OAc)_3$ (11.9 μmol, 5 equiv) were added. The mixture was subjected to sonication for a few minutes. The ^{1}H NMR spectrum recorded at 298 K showed the formation of **2$_{Bi}$·Bi(OAc)$_2$** as the major species (95%; see above).

The complex **2(BiOAc)$_2$** was prepared following the protocol used for **2$_{Bi}$·Bi(OAc)$_2$** except that no DIPEA was added. After sonication, the ^{1}H spectrum recorded at 298 K showed the formation of **2(BiOAc)$_2$** as the major species (85%; see above).

The complex **2$_{Bi}$·PbOAc** was prepared from a solution of 3.5 mg of **2$_{Bi}$** (2.39 μmol) in 500 μL of DMSO-d_6 to which 40 μL (2.38 μmol, 1 equiv) of a stock solution of $Pb(OAc)_2{\cdot}3H_2O$ (11.3 mg in 500 μL of DMSO-d_6) was added. The ^{1}H spectrum recorded at 298 K showed the quantitative formation of **2$_{Bi}$·PbOAc**.

dx.doi.org/10.1021/ja307349d | J. Am. Chem. Soc. 2012, 134, 16017–16032

Assignment of the NMR Signals of Complexes 2_{Pb}·PbOAc, 2_{Bi}·Bi(OAc)$_2$, 2(BiOAc)$_2$, and 2_{Bi}·PbOAc. ***2_{Pb}·PbOAc.*** ^{1}H NMR (9:1 $CDCl_3/CD_3OD$, 15 equiv of DIPEA, 223 K, 500 MHz): δ 9.50 (d, 1H, J = 4 Hz, $H_{\beta pyr}$), 9.41 (d, 1H, J = 4 Hz, $H_{\beta pyr}$), 9.27 (d, 1H, J = 9 Hz, HAr_{meso}), 9.10 (d, 1H, J = 4 Hz, $H_{\beta pyr}$), 9.08 (d, 1H, J = 4 Hz, $H_{\beta pyr}$), 9.00 (d, 1H, J = 4 Hz, $H_{\beta pyr}$), 8.96 (d, 1H, J = 4 Hz, $H_{\beta pyr}$), 8.94 (d, 1H, J = 8 Hz, HAr_{meso}), 8.92−8.85 (m, 5H, $2H_{\beta pyr}$ + $3HAr_{meso}$), 8.64 (d, 1H, J = 8 Hz, HAr_{meso}), 8.14 (d, 1H, J = 8 Hz, HAr_{meso}), 7.90−7.82 (m, 3H, HAr_{meso}), 7.78 (t, 1H, J = 8 Hz, HAr_{meso}), 7.77 (t, 1H, J = 8 Hz, HAr_{meso}), 7.72 (t, 1H, J = 8 Hz, HAr_{meso}), 7.69 (t, 1H, J = 8 Hz, HAr_{meso}), 7.50 (t, 1H, J = 8 Hz, HAr_{meso}), 7.48 (t, 1H, J = 8 Hz, HAr_{meso}), 7.30 (d, 1H, J = 8 Hz, HAr_{strap}), 7.25 (d, 1H, J = 8 Hz, HAr_{strap}), 7.18 (d, 1H, J = 8 Hz, HAr_{strap}), 7.08 (d, 1H, J = 8 Hz, HAr_{strap}), 6.95 (t, 1H, J = 8 Hz, HAr_{strap}), 6.91 (t, 1H, J = 8 Hz, HAr_{strap}), 6.89 (t, 1H, J = 8 Hz, HAr_{strap}), 6.88 (t, 1H, J = 8 Hz, HAr_{strap}), 6.86 (d, 1H, J = 8 Hz, HAr_{strap}), 6.80 (d, 1H, J = 8 Hz, HAr_{strap}), 6.78 (d, 1H, J = 8 Hz, HAr_{strap}), 6.73 (d, 1H, J = 8 Hz, HAr_{strap}), 6.02 (s, 1H, HAr_{strap}), 5.74 (s, 1H, HAr_{strap}), 5.37 (s, 1H, HAr_{strap}), 5.27 (s, 1H, HAr_{strap}), 2.48 (d, 1H, J = 9 Hz, CH_{benz}), 2.39 (d, 1H, J = 9 Hz, CH_{benz}), 2.34 (d, 1H, J = 9 Hz, CH_{benz}), 2.27 (d, 1H, J = 9 Hz, CH_{benz}), 2.20 (m, 1H, CH_{benz}), 2.04 (m, 1H, CH_{benz}), 1.80 (m, 1H, CH_{benz}), 1.71 (m, 1H, CH_{benz}), 1.48 (m, 1H, CHCO), 1.31 (m, 1H, CHCO), 0.24 (s, 3H, H_{AcO^-}).

2_{Bi}·Bi(OAc)$_2$. ^{1}H NMR (DMSO-d_6, 15 equiv of DIPEA, 298 K, 500 MHz): δ 10.33 (s, 1H, NHCO), 10.12 (s, 1H, NHCO), 9.88 (s_b, 1H, NHCO), 9.85 (s_b, 1H, NHCO), 9.37 (d, 1H, J = 9 Hz, HAr_{meso}), 9.34 (d, 1H, J = 9 Hz, HAr_{meso}), 9.30 (m, 2H, $H_{\beta pyr}$ + HAr_{meso}), 9.26 (d, 1H, J = 9 Hz, HAr_{meso}), 9.15 (d, 1H, J = 4 Hz, $H_{\beta pyr}$), 9.02 (d, 1H, J = 4 Hz, $H_{\beta pyr}$), 8.99 (d, 1H, J = 4 Hz, $H_{\beta pyr}$), 8.95 (d, 1H, J = 4 Hz, $H_{\beta pyr}$), 8.92 (d, 1H, J = 8 Hz, HAr_{meso}), 8.85 (d, 1H, J = 4 Hz, $H_{\beta pyr}$), 8.82 (d, 1H, J = 4 Hz, $H_{\beta pyr}$), 8.80 (d, 1H, J = 4 Hz, $H_{\beta pyr}$), 8.64 (d, 1H, J = 7 Hz, HAr_{meso}), 7.94−7.85 (m, 3H, HAr_{meso}), 7.84−7.76 (m, 3H, HAr_{meso}), 7.75−7.67 (m, 2H, HAr_{meso}), 7.53 (t, 1H, J = 7 Hz, HAr_{meso}), 7.49 (t, 1H, J = 7 Hz, HAr_{meso}), 7.30−7.21 (m, 2H, HAr_{strap}), 7.24 (d, 1H, J = 8 Hz, HAr_{strap}), 7.17 (d, 1H, J = 8 Hz, HAr_{strap}), 7.04−6.97 (m, 2H, HAr_{strap}), 6.96 (d, 1H, J = 8 Hz, HAr_{strap}), 6.94−6.89 (m, 3H, HAr_{strap}), 6.86 (d, 1H, J = 8 Hz, HAr_{strap}), 6.82 (d, 1H, J = 8 Hz, HAr_{strap}), 5.91 (s, 1H, HAr_{strap}), 5.70 (s, 1H, HAr_{strap}), 5.52 (s, 1H, HAr_{strap}), 5.48 (s, 1H, HAr_{strap}), 2.57 (m, 1H, CH_{benz}), 2.39 (m, 1H, CH_{benz}), 2.28 (m, 1H, CH_{benz}), 2.09 (m, 1H, CH_{benz}), 1.87 (m, 1H, CH_{benz}), 1.83 (m, 1H, CH_{benz}), 1.59 (m, 2H, CH_{benz}), 1.34 (m, 1H, CHCO), 1.26 (m, 1H, CHCO), 0.39 (s, 3H, H_{AcO^-}), 0.16 (s, 3H, H_{AcO^-}).

2(BiOAc)$_2$. ^{1}H NMR (DMSO-d_6, 298 K, 500 MHz): δ 9.66 (s, 2H, NHCO), 9.45 (s, 2H, $H_{\beta pyr}$), 9.38 (d, 2H, J = 8 Hz, HAr_{meso}), 9.23 (d, 2H, J = 8 Hz, HAr_{meso}), 9.18 (d, 2H, J = 4 Hz, $HAr_{\beta pyr}$), 9.11 (d, 2H, J = 4 Hz, $HAr_{\beta pyr}$), 9.07 (s, 2H, $H_{\beta pyr}$), 8.89 (d, 2H, J = 8 Hz, HAr_{meso}), 8.61 (s, 2H, NHCO), 7.98 (t, 2H, J = 8 Hz, HAr_{meso}), 7.90 (t, 2H, J = 8 Hz, HAr_{meso}), 7.85 (t, 2H, J = 7 Hz, HAr_{meso}), 7.78 (d, 2H, J = 7 Hz, HAr_{meso}), 7.58 (t, 2H, J = 7 Hz, HAr_{meso}), 7.33 (d, 2H, J = 8 Hz, HAr_{strap}), 7.26 (d, 2H, J = 8 Hz, HAr_{strap}), 7.07 (t, 2H, J = 8 Hz, HAr_{strap}), 7.03 (t, 2H, J = 8 Hz, HAr_{strap}), 7.01 (d, 2H, J = 8 Hz, HAr_{strap}), 6.94 (d, 2H, J = 8 Hz, HAr_{strap}), 5.90 (s, 2H, HAr_{strap}), 5.23 (s, 2H, HAr_{strap}), 2.68 (d, 2H, J = 12 Hz, CH_{benz}), 2.54 (d, 2H, J = 12 Hz, CH_{benz}), 2.10 (t, 2H, J = 12 Hz, CH_{benz}), 1.74 (t, 2H, J = 12 Hz, CH_{benz}), 1.46 (m, 2H, CHCO), 0.06 (s, 6H, H_{AcO^-}).

2_{Bi}·PbOAc. ^{1}H NMR (DMSO-d_6, 298 K, 500 MHz): δ 10.1−6.7 (complex region with broad and overlapped signals, 40H, $H_{\beta pyr}$ + HAr_{meso} + HAr_{strap}; see the SI), 5.91 (s, 1H, HAr_{strap}), 5.60 (s, 1H, HAr_{strap}), 5.43 (s, 1H, HAr_{strap}), 5.16 (s, 1H, HAr_{strap}), 2.52 (m, 1H, CH_{benz}), 2.38 (m, 1H, CH_{benz}), 2.15−1.75 (m, 5H, CH_{benz}), 1.61 (m, 1H, CH_{benz}), 1.49 (m, 1H, CHCO), 1.15 (m, 1H, CHCO), 0.36 (s_b, 3H, H_{AcO^-}).

HRMS Analysis of 2_{Pb}·PbOAc. Complex 2_{Pb}·PbOAc was prepared from a DMSO solution of **2**, DIPEA (15 equiv), and $Pb(OAc)_2$ (2 equiv). The deep-green solution was evaporated to dryness under high vacuum. The residue was solubilized in dichloromethane and subjected to HRMS analysis (ESI-TOF, negative-ion mode): calcd for $C_{82}H_{57}N_8O_{10}Pb_2$ [$M^{\bullet-}$], m/z 1729.3740; found, m/z 1729.3752.

Preparation of an Analytical Sample of 2_{Bi}·Bi(OAc)$_2$. Complex 2_{Bi} (32 mg, 21.8 μmol) was dissolved in 3 mL of $CHCl_3$, and $Bi(OAc)_3$ (42 mg, 108 μmol) was added. The mixture was sonicated for ∼5 min and then stirred for 1 h at room temperature. The excess bismuth was removed by filtration on a pad of Celite. Pentane was added to the eluate, and the green precipitate was isolated by centrifugation. The solid was solubilized in ∼3 mL of $CHCl_3$, and the solution was filtered a second time on a pad of Celite. Upon precipitation with pentane and centrifugation, **2_{Bi}·Bi(OAc)$_2$** was obtained as a green solid in 82% yield (32 mg). ^{1}H NMR ($CDCl_3$, 298 K, 500 MHz): δ 9.81 (d, 1H, J = 4 Hz, $H_{\beta pyr}$), 9.61 (d, 1H, J = 4 Hz, $H_{\beta pyr}$), 9.45 (d, 1H, J = 4 Hz, $H_{\beta pyr}$), 9.43 (d, 1H, J = 7 Hz, HAr_{strap}), 9.41 (d, 1H, J = 4 Hz, $H_{\beta pyr}$), 9.40 (s, 1H, NHCO), 9.38 (d, 1H, J = 8 Hz, HAr_{strap}), 9.35 (d, 1H, J = 4 Hz, $H_{\beta pyr}$), 9.28 (s, 1H, NHCO), 9.27 (d, 1H, J = 4 Hz, $H_{\beta pyr}$), 9.24 (d, 1H, J = 8 Hz, HAr_{strap}), 9.16 (d, 1H, J = 4 Hz, $H_{\beta pyr}$), 9.14 (d, 1H, J = 4 Hz, $H_{\beta pyr}$), 9.12 (d, 1H, J = 8 Hz, HAr_{strap}), 8.69 (d, 1H, J = 8 Hz, HAr_{strap}), 8.47 (d, 1H, J = 8 Hz, HAr_{strap}), 8.45 (s, 1H, NHCO), 8.27 (s, 1H, NHCO), 7.99 (t, 1H, J = 7 Hz, HAr_{meso}), 7.95 (t, 1H, J = 7 Hz, HAr_{meso}), 7.93−7.88 (m, 4H, HAr_{meso}), 7.72 (t, 1H, J = 7 Hz, HAr_{meso}), 7.70 (t, 1H, J = 7 Hz, HAr_{meso}), 7.56 (t, 1H, J = 8 Hz, HAr_{meso}), 7.52 (t, 1H, J = 8 Hz, HAr_{meso}), 7.44 (d, 1H, J = 8 Hz, HAr_{strap}), 7.39 (m, 2H, HAr_{strap}), 7.31 (d, 1H, J = 8 Hz, HAr_{strap}), 7.01−6.94 (m, 3H, HAr_{strap}), 6.90 (t, 1H, J = 8 Hz, HAr_{strap}), 6.83 (d, 1H, J = 8 Hz, HAr_{strap}), 6.80 (d, 1H, J = 8 Hz, HAr_{strap}), 6.76 (d, 1H, J = 8 Hz, HAr_{strap}), 6.69 (d, 1H, J = 8 Hz, HAr_{strap}), 5.59 (s, 1H, HAr_{strap}), 5.57 (s, 1H, HAr_{strap}), 5.40 (s, 1H, HAr_{strap}), 5.30 (s, 1H, HAr_{strap}), 2.50 (d, 1H, J = 14 Hz, CH_{benz}), 2.47 (d, 1H, J = 14 Hz, CH_{benz}), 2.35 (d, 1H, J = 14 Hz, CH_{benz}), 2.32 (d, 1H, J = 9 Hz, CH_{benz}), 1.95 (t, 1H, J = 12 Hz, CH_{benz}), 1.87 (t, 1H, J = 12 Hz, CH_{benz}), 1.64 (t, 1H, J = 12 Hz, CH_{benz}), 1.47−1.31 (m, 3H, CH_{benz} + CHCO), 0.68 (s, 3H, H_{AcO^-}), 0.52 (s, 3H, H_{AcO^-}). Anal. Calcd for $C_{84}H_{60}Bi_2N_8O_{12}\cdot 4H_2O$: C, 54.14; H, 3.68; N, 6.01. Found: C, 53.97; H, 3.33; N, 5.96.

Crystal Data for Complex 2_{Bi}·Bi(OAc)$_2$. $C_{85.69}H_{65.30}Bi_{1.92}Cl_6N_8O_{13.53}$, M = 2034.79; Bruker-AXS APEXII diffractometer, Mo Kα radiation (λ = 0.71073 Å), T = 150(2) K; triclinic, $P\bar{1}$; a = 13.6220(6) Å, b = 17.1160(8) Å, c = 19.5296(9) Å, α = 101.445(2)°, β = 93.541(2)°, γ = 94.140(2)°; V = 4437.7(4) Å^3, Z = 2, d = 1.523 g cm^{-3}, μ = 4.047 mm^{-1}. The structure was solved by direct methods using SIR97[37] and then refined with full-matrix least-squares methods based on F^2 using SHELXL-97[38] with the aid of WINGX.[39] The contribution of the disordered solvents to the calculated structure factors was estimated using the BYPASS algorithm[40] as implemented in the SQUEEZE option in PLATON.[41] A new data set, free of solvent contributions, was then used in the final refinement. All non-hydrogen atoms were refined with anisotropic atomic displacement parameters. H atoms were finally included in their calculated positions. A final refinement on F^2 with 19 365 unique intensities and 996 parameters converged at $wR(F^2)$ = 0.1635 [$R(F)$ = 0.0633] for 11 401 observed reflections with $I > 2\sigma(I)$. The crystallographic data were deposited with the Cambridge Crystallographic Data Centre as entry CCDC 893282.

Crystal Data for Complex 2_{Bi}·PbOAc. $C_{88}H_{75}BiN_8O_{13}PbS_3$, M = 1964.91; Bruker-AXS APEXII diffractometer, Mo Kα radiation (λ = 0.71073 Å), T = 150(2) K; monoclinic, $C2/c$; a = 44.3331(12) Å, b = 16.6415(4) Å, c = 31.6038(10) Å, β = 115.3480(10)°; V = 21071.5(10) Å^3, Z = 8, d = 1.239 g cm^{-3}, μ = 3.376 mm^{-1}. The structure was solved by direct methods using SIR97[37] and then refined with full-matrix least-squares methods based on F^2 using SHELXL-97[38] with the aid of WINGX.[39] The contribution of the disordered solvents to the calculated structure factors was estimated using the BYPASS algorithm[40] as implemented in the SQUEEZE option in PLATON.[41] A new data set, free of solvent contributions, was then used in the final refinement. All non-hydrogen atoms were refined with anisotropic atomic displacement parameters. H atoms were finally included in their calculated positions. A final refinement on F^2 with 24 047 unique intensities and 1040 parameters converged at $wR(F^2)$ = 0.1262 [$R(F)$ = 0.0505]) for 17 764 observed reflections with $I > 2\sigma(I)$. The crystallographic data were deposited with the Cambridge Crystallographic Data Centre as entry CCDC 845671.

dx.doi.org/10.1021/ja307349d | J. Am. Chem. Soc. 2012, 134, 16017−16032

■ ASSOCIATED CONTENT

Supporting Information

2D NMR spectra of complexes $\mathbf{2}_{Pb}$·**PbOAc**, $\mathbf{2}_{Bi}$·**Bi(OAc)$_2$**, and $\mathbf{2}_{Bi}$·**PbOAc**; calculation of the free Gibbs energy for the Newton's cradle-like motion of Pb(II) cations in $\mathbf{2}_{Pb}$·**PbOAc**; ^{1}H NMR spectra related to the acid−base-controlled formation of $\mathbf{2}_{Bi}$·**PbOAc**; comparison of the X-ray structures of $\mathbf{2}_{Bi}$·**Bi(OAc)$_2$**, $\mathbf{2}_{Bi}$·**PbOAc**, $\mathbf{1}_{Pb}$·**PbOAc**, and $\mathbf{2}_{Bi}$; and crystallographic data (CIF). This material is available free of charge via the Internet at http://pubs.acs.org.

■ AUTHOR INFORMATION

Corresponding Author

stephane.legac@univ-rennes1.fr; bernard.boitrel@univ-rennes1.fr

Notes

The authors declare no competing financial interest.

■ ACKNOWLEDGMENTS

Financial support from "La ligue contre le cancer" is gratefully acknowledged.

■ REFERENCES

(1) Champin, B.; Mobian, P.; Sauvage, J.-P. *Chem. Soc. Rev.* **2007**, *36*, 358−366.

(2) (a) Coskun, A.; Banaszak, M.; Astumian, R. D.; Stoddart, J. F.; Grzybowski, B. A. *Chem. Soc. Rev.* **2012**, *41*, 19−30. (b) Balzani, V.; Credi, A.; Venturi, M. *Molecular Devices and Machines: A Journey into the Nanoworld*; Wiley-VCH: Weinheim, Germany, 2003. (c) *Molecular Switches*; Feringa, B. L., Ed.; Wiley-VCH: Weinheim, Germany, 2001; pp 281−307.

(3) (a) Amendola, V.; Fabbrizzi, L.; Licchelli, M.; Mangano, C.; Pallavicini, P.; Parodi, L.; Poggi, A. *Coord. Chem. Rev.* **1999**, *190−192*, 649−669. (b) Amendola, V.; Fabbrizzi, L.; Licchelli, M.; Mangano, C.; Pallavicini, P. *Acc. Chem. Res.* **2001**, *34*, 488−493.

(4) (a) Zelikovich, L.; Libman, J.; Shanzer, A. *Nature* **1995**, *374*, 790−792. (b) Belle, C.; Pierre, J.-L.; Saint-Aman, E. *New J. Chem.* **1998**, *22*, 1399−1402. (c) Ward, T. R.; Lutz, A.; Parel, S. P.; Ensling, J.; Gütlich, P.; Buglyó, P.; Orvig, C. *Inorg. Chem.* **1999**, *38*, 5007−5017.

(5) (a) Ikeda, A.; Tsudera, T.; Shinkai, S. *J. Org. Chem.* **1997**, *62*, 3568−3574. (b) Amendola, V.; Fabbrizzi, L.; Mangano, C.; Pallavicini, P.; Perotti, A.; Taglietti, A. *J. Chem. Soc., Dalton Trans.* **2000**, 185−189. (c) Lodeiro, C.; Parola, A. J.; Pina, F.; Bazzicalupi, C.; Bencini, A.; Bianchi, A.; Giorgi, C.; Masotti, A.; Valtancoli, B. *Inorg. Chem.* **2001**, *40*, 2968−2975.

(6) Fabbrizzi, L.; Foti, F.; Patroni, S.; Pallavicini, P.; Taglietti, A. *Angew. Chem., Int. Ed.* **2004**, *43*, 5073−5077.

(7) Colasson, B.; Le Poul, N.; Le Mest, Y.; Reinaud, O. *J. Am. Chem. Soc.* **2010**, *132*, 4393−4398.

(8) Beletskaya, I.; Tyurin, V. S.; Tsivadze, A. Y.; Guilard, R.; Stern, C. *Chem. Rev.* **2009**, *109*, 1659−1713.

(9) For selected examples, see: (a) Tabata, M.; Miyata, W.; Nahar, N. *Inorg. Chem.* **1995**, *34*, 6492−6496. (b) Grant, C., Jr.; Hambright, P. *J. Am. Chem. Soc.* **1969**, *91*, 4195−4198.

(10) (a) Buchler, J. W. In *Porphyrins and Metalloporphyrins*; Smith, K. M., Ed.; Elsevier: Amsterdam, 1975; pp 157−231. (b) Sanders, J. K. M.; Bampos, N.; Clyde-Watson, Z.; Darling, S. L.; Hawley, J. C.; Kim, H.-J.; Mak, C. C.; Webb, S. J. In *The Porphyrin Handbook*; Kadish, K. M., Smith, K. M., Guilard, R., Eds.; Academic Press: Boston, 2000; Vol. 3, pp 1−48.

(11) (a) Tanaka, H.; Ikeda, T.; Takeuchi, M.; Sada, K.; Shinkai, S.; Kawai, T. *ACS Nano* **2011**, *5*, 9575−9582. (b) Buchler, J. W.; Ng, D. K. P. In *The Porphyrin Handbook*; Kadish, K. M., Smith, K. M., Guilard, R., Eds.; Academic Press: Boston, 2000; Vol. 3, pp 245−294.

(12) (a) Mashiko, T.; Reed, C. A.; Haller, K. J.; Scheidt, W. R. *Inorg. Chem.* **1984**, *23*, 3192−3196. (b) Ciurli, S.; Gambarotta, S.; Floriani, C.; Chiesi-Villa, A.; Guasfini, C. *Angew. Chem., Int. Ed. Engl.* **1986**, *25*, 553−554. (c) Arnold, J.; Dawson, D. Y.; Hoffman, C. C. *J. Am. Chem. Soc.* **1993**, *115*, 2707−2713.

(13) Tsutsui, M.; Hrung, C. P.; Ostfeld, D.; Srivastava, T. S.; Cullen, D. L.; Meyer, E. F., Jr. *J. Am. Chem. Soc.* **1975**, *97*, 3952−3965.

(14) Lai, J.-J.; Khademi, S.; Meyer, E. F., Jr.; Cullen, D. L.; Smith, K. M. *J. Porphyrins Phthalocyanines* **2001**, *5*, 621−627.

(15) For reviews, see: (a) Sessler, J. L.; Tomat, E. *Acc. Chem. Res.* **2007**, *40*, 371−379. (b) Seito, S.; Osuka, A. *Angew. Chem., Int. Ed.* **2011**, *50*, 4342−4373.

(16) (a) Lemon, C. M.; Brothers, P. J.; Boitrel, B. *Dalton Trans.* **2011**, *40*, 6591−6609. (b) Le Gac, S.; Boitrel, B. *J. Porphyrins Phthalocyanines* **2012**, *16*, 537−544.

(17) Halime, Z.; Lachkar, M.; Roisnel, T.; Furet, E.; Halet, J.-F.; Boitrel, B. *Angew. Chem., Int. Ed.* **2007**, *46*, 5120−5124.

(18) Motreff, N.; Le Gac, S.; Luhmer, M.; Furet, E.; Halet, J.-F.; Roisnel, T.; Boitrel, B. *Angew. Chem., Int. Ed.* **2011**, *50*, 1560−1564.

(19) For a review covering supramolecular assemblies with main-group elements, see: Pitt, M. A.; Johnson, D. W. *Chem. Soc. Rev.* **2007**, *36*, 1441−1453.

(20) Le Gac, S.; Najjari, B.; Fusaro, L.; Roisnel, T.; Dorcet, V.; Luhmer, M.; Furet, E.; Halet, J.-F.; Boitrel, B. *Chem. Commun.* **2012**, *48*, 3724−3726.

(21) $\mathbf{1}_{Pb}$ ($\mathbf{1}^{Pb}$) refers to an Pb(II) cation coordinated out-of-plane in an *outside* (*inside*) position relative to the strap.

(22) For clarity, the nomenclature used in the case of Pb(II) complexes of **1** (i.e., $\mathbf{1}_{Pb}/\mathbf{1}^{Pb}$; see ref 21) is used in the case of dissymmetric complexes of **2**. Hence, $\mathbf{2}_{Bi}$ (with Bi subscripted) corresponds to an OOP Bi(III) cation arbitrarily represented as bound to the lower side of the porphyrin, as drawn in Figure 1.

(23) We also recently reported the influence of lead on the kinetics of bismuth insertion in **2**. See: Le Gac, S.; Najjari, B.; Motreff, N.; Remaud-Le Saec, P.; Faivre-Chauvet, A.; Dimanche-Boitrel, M.-T.; Morgenstern, A.; Bruchertseifer, F.; Lachkar, M.; Boitrel, B. *Chem. Commun.* **2011**, *47*, 8554−8556. This aspect will not be discussed herein.

(24) The reasons for such an impressive cooperativity are not yet understood. Two Hg(II) cations were also bound into **2** according to a positive cooperative process, but only in the absence of a base (see ref 18). For an example of insertion of a metal ion [e.g., Ag(I)] into an expanded porphyrin macrocycle with positive cooperativity, see: Sessler, J. L.; Tomat, E.; Lynch, V. M. *J. Am. Chem. Soc.* **2006**, *128*, 4184−4185.

(25) See the Experimental Section.

(26) As expected, the ROESY spectrum of $\mathbf{2}_{Pb}$·**PbOAc** recorded at low temperature revealed exchange correlations between peaks involved the coalescence process (e.g., $H_a \leftrightarrow H_{a'}$; see the SI).

(27) Pb(acac)$_2$ (acac = acetylacetonate) was chosen because of its good solubility in 9:1 $CDCl_3/CD_3OD$. Under those conditions, the acac ligand does not compete with acetate, and the complex $\mathbf{2}_{Pb}$·**PbOAc** is readily formed.

(28) A Newton's cradle, named after Sir Isaac Newton, is a device used to illustrate conservation of momentum and energy. It consists of a series of equal pendulums in a row, and a swinging motion is induced by the release of a sphere pulled away at one extremity. Collision with a second sphere sends the momentum through the series of spheres, causing the opposite swinging motion of a sphere at the other extremity of the device. Swinging back and collision with the series of resting spheres leads to the reverse swinging motion of the first sphere, and this coupled back-and-forth motion repeats until it wears down.

(29) Anelli, P. L.; Spencer, N.; Stoddart, J. F. *J. Am. Chem. Soc.* **1991**, *113*, 5131−5133.

(30) Ikeda, A.; Shinkai, S. *J. Am. Chem. Soc.* **1994**, *116*, 3102−3110.

(31) Assignment of the NHCO signals in the mono- and bimetallic complexes was performed on the basis of 2D ROESY NMR spectra. However, the protons labeled "a" and "b" could not be unambiguously

distinguished from each other. They differ by the spatial orientation of the carboxylic group on the opposite side.
(32) The complex crystallized as a mixture of the dinuclear complex $\mathbf{2}_{Bi}$·$\mathbf{Bi(OAc)_2}$ (92.25%) and the mononuclear complex $\mathbf{2}_{Bi}$ (7.75%). In the latter, the Bi atom was disordered over two positions on each side of the macrocycle, one of them being confused with the OOP Bi atom of the dinuclear complex.
(33) (a) Rogers, R. D.; Bond, A. H.; Aguinaga, S. *J. Am. Chem. Soc.* **1992**, *114*, 2960−2967. (b) Rogers, R. D.; Bond, A. H.; Aguinaga, S.; Reyes, A. *J. Am. Chem. Soc.* **1992**, *114*, 2967−2977.
(34) From the X-ray crystal structure, the NH_a−H_a and NH_b−H_b distances range from 2.324 to 2.758 Å, whereas the NH_a−$H_{a'}$ and NH_b−$H_{b'}$ distances range from 9.491 to 6.119 Å.
(35) Detailed studies of the influence of the base, the solvent, and the temperature will be described elsewere.
(36) Al-Karadaghi, S.; Franco, R.; Hansson, M.; Shelnutt, J. A.; Isaya, G.; Ferreira, G. C. *Trends Biochem. Sci.* **2006**, *31*, 135−142.
(37) Altomare, A.; Burla, M. C.; Camalli, M.; Cascarano, G.; Giacovazzo, C.; Guagliardi, A.; Moliterni, A. G. G.; Polidori, G.; Spagna, R. *J. Appl. Crystallogr.* **1999**, *32*, 115−119.
(38) Sheldrick, G. M. *Acta Crystallogr., Sect. A* **2008**, *64*, 112−122.
(39) Farrugia, L. J. *J. Appl. Crystallogr.* **1999**, *32*, 837−838.
(40) Van der Sluis, P.; Spek, A. L. *Acta Crystallogr., Sect. A* **1990**, *46*, 194−201.
(41) Spek, A. L. *J. Appl. Crystallogr.* **2003**, *36*, 7−13.